Comparing Reactor Types for Saponification

Final Report

Reactive Process Engineering Lab 401

Tuesday B-2

Team Members:

Taylor Doliveira- Shaffer

James Hughes

Michael Luketich

Kyler Madara

Kaitlin Muzic

Nicholas Yuhas

Table of Contents

NOMENCLATURE **1**

1.0 INTRODUCTION AND BACKGROUND **3**

2.0 EXPERIMENTAL METHODOLOGY **8**

2.1 EQUIPMENT AND APPARATUS 8

2.2 EXPERIMENTAL VARIABLES AND KEY MEASURES 13

3.0 RESULTS **14**

3.1 THERMODYNAMIC ANALYSIS 14

3.2 BATCH REACTOR 15

3.3 OLD CSTR 20

3.4 NEW CSTR 24

3.5 PFR 26

4.0 ANALYSIS AND DISCUSSION **34**

5.0 SUMMARY AND CONCLUSIONS **40**

6.0 REFERENCES **42**

7.0 APPENDIX **43**

7.1 APPENDIX – SAMPLE CALCULATIONS 43

7.1.1 Thermodynamic Analysis *43*

7.1.2 Batch *44*

7.1.3 Old CSTR *48*

7.1.3.a. Specific Conductance 48

7.1.3.b. Conversion 48

7.1.3.c. Residence time 49

7.1.3.d. Rate Constant 49

7.1.3.e. Activation Energy 50

7.1.3.f. Productivity 51

7.1.4 New CSTR *51*

7.1.4.a. Conductance 51

7.1.4.b. Conversion 52

7.1.4.c Concentration 53

7.1.4.d Residence Time 53

7.1.4.f. Productivity 53

7.1.5 PFR *54*

7.1.5.a. Specific Conductance 54

7.1.5.b. Conversion 54

7.1.5.c. Residence time 54

7.1.5.d. Rate Constant 55

7.1.5.e. Activation Energy 55

7.1.5.f. PFR Equations: 56

7.1.5.g. Productivity 56

Nomenclature

Symbol	Term	Units
ΔH_R	Enthalpy of Reaction	$\frac{kJ}{mol}$
ΔH_{NaAc}	Enthalpy of NaAc formation	$\frac{kJ}{mol}$
ΔH_{EtOH}	Enthalpy of EtOH formation	$\frac{kJ}{mol}$
ΔH_{NaOH}	Enthalpy of NaOH formation	$\frac{kJ}{mol}$
ΔH_{EtAc}	Enthalpy of EtAc formation	$\frac{kJ}{mol}$
ΔG_R	Standard Gibb's Free Energy of Reaction	$\frac{kJ}{mol}$
ΔG_{NaAc}	Gibb's Free Energy of NaAc formation	$\frac{kJ}{mol}$
ΔG_{EtOH}	Gibb's Free Energy of EtOH formation	$\frac{kJ}{mol}$
ΔG_{NaOH}	Gibb's Free Energy of NaOH formation	$\frac{kJ}{mol}$
ΔG_{EtAc}	Gibb's Free Energy of EtAc formation	$\frac{kJ}{mol}$
K_{eq}	Equilibrium Constant	-
R	Ideal Gas Constant	$\frac{J}{mol*K}$
k	Reaction Rate Coefficient	$\frac{L}{mol*s}$
P	Productivity	$\frac{mol\ NaAc}{L*min}$
P_{single}	productivity for single CSTR	$\frac{mol\ NaAc}{L*min}$
$P_{overall}$	overall productivity for two CSTRs in series	$\frac{mol\ NaAc}{L*min}$
V_{NaOH}	Volume of Feed NaOH	$\frac{mL}{min}$
λ_j	specific conductance of species j, where j = NaAc or NaOH	$\frac{mS*L}{mol}$
κ	experimental conductivity	mS
$\kappa_{j,std}$	standard conductivity of species j, where j = NaAc or NaOH	mS
$\alpha_{j,std}$	lambda correction	$\frac{mS}{℃}$
T	Experimental Temperature	K
$T_{j,std}$	standard temperature of species j, where j = NaAc or NaOH	K
$C_{j,std}$	standard concentration of species j, where j = NaAc or NaOH	$\frac{mol}{L}$
X	conversion	-
X_{single}	conversion for a single CSTR	-
X_1	conversion for 1st CSTR in series	-
X_2	conversion for 2nd CSTR in series	-

$X_{overall}$	overall conversion for two CSTRs in series	-
$C_{NaOH,0}$	initial concentration of NaOH	$\frac{mol}{L}$
$C_{NaOH,1}$	concentration of NaOH after 1st CSTR in series	$\frac{mol}{L}$
$C_{NaAc,1}$	concentration of NaAc after 1st CSTR in series	$\frac{mol}{L}$
$C_{NaOH,2}$	concentration of NaOH after 2nd CSTR in series	$\frac{mol}{L}$
τ	residence time	min
τ_{single}	residence time for single CSTR	min
$\tau_{overall}$	overall residence time for two CSTRs in series	min
V	volume of reactor	L
V_{single}	volume of single CSTR	L
V_1	volume of 1st CSTR in series	L
V_2	volume of 2nd CSTR in series	L
ύ	volumetric flow rate	$\frac{mL}{min}$
F_{single}	total volumetric flow rate for single CSTR	$\frac{mL}{min}$
F_1	total volumetric flow rate for 1st CSTR in series	$\frac{mL}{min}$
F_2	total volumetric flow rate for 2nd CSTR in series	$\frac{mL}{min}$
k_f	rate constant (L/mol*min)	$\frac{L}{mol*min}$
E_a	Activation Energy	$\frac{kJ}{mol}$
u	Linear Velocity	$\frac{m}{s}$

1.0 Introduction and Background

Reactions, whether chemical or physical, occur everywhere; however, a chemical reactor is a device properly designed to allow reactions to occur under controlled conditions to achieve specified products. Hence, it is inarguably the single most important factor in the design phase of a chemical process. The design of a reactor must be finely tuned so that a mechanism suits the necessities of the process to be carried out. Since a reactor depends significantly on the nature of the materials in both the feed and the product stream, the reactor may take a wide range of forms. Thus, a full comprehension of a reactor's design as well as the working mechanism is key to correctly conducting a successful chemical process.

In this experiment, an exothermic reaction known as saponification occurred. This process is used to manufacture soap from fats and lye. In this process, a triglyceride (ester) is reacted with a strong base such as potassium or sodium hydroxide, which accelerates cleavage of the ester bond to form glycerol (alcohol) and fatty acid salts (carboxylic acid). In Figure 1, the mechanism of base hydrolysis of a generic ester is demonstrated.

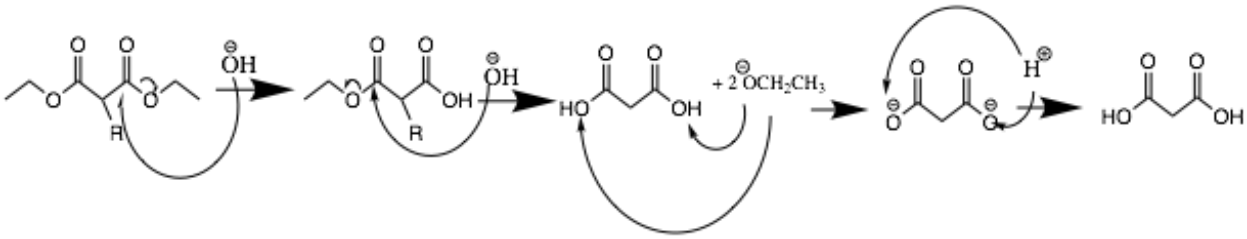


Fig. 1. Base Hydrolysis: Saponification of a Generic Ester

In this mechanism, the hydroxide anion adds to the electrophilic carbonyl group of the ester, breaking the pi-bond and creating a tetrahedral intermediate. The intermediate readily collapses, reforming the carbon-oxygen bond, which results in the loss of the alkoxide. Next, the alkoxide functions as a strong base and deprotonates the carboxylic acid. Thus, acidic work-up is used to obtain the carboxylic acid from the reaction.

In theory, the rate of reaction is defined as the rate of consumption of reactants or the rate of formation of products. Below, the saponification reaction is represented, which provides a blueprint to express the rate of reaction.

$$\underset{(ethyl\ acetate)}{CH_3CO_2C_2H_5} + \underset{(sodium\ hydroxide)}{Na^+OH^-} \rightleftarrows \underset{(ethanol)}{C_2H_5OH} + \underset{(sodium\ acetate)}{CH_3CO_2{}^-Na^+}$$

Thus, the rate of reaction for the saponification reaction can be expressed as follows.

$$r_{EtAc} = k_r C_{EtOH} C_{NaAc} - k_f C_{EtAc} C_{NaOH} \quad (1)$$

The hydrolysis of ethyl acetate is represented in the overall second order reversible reaction, where the forward and backward reactions were combined. The forward reaction for the specific reaction rate coefficient, at moderate temperatures, is significantly higher than the specific reaction rate coefficient of the reverse reaction; thus, pushing the reaction equilibrium towards the product side.

After the reaction rate law is established, the reaction concentrations of both the reactant and products were determined using conductivity. Since conductivity relies on the ion concentration and the specific conductance of each ion present, an overall simplified equation was produced, which assumed that both sodium hydroxide and sodium acetate were fully dissociated in solution.

$$\kappa = (\lambda_{NaOH} \times C_{NaOH}) + (\lambda_{NaAc} \times C_{NaAc}) \quad (2)$$

The specific conductance of sodium hydroxide and sodium acetate was developed, exhibiting a linear relationship to temperature. Therefore, specific conductance was calculated at each respective reactor temperature.

$$\lambda_{NaOH} = \frac{\kappa_{NaOH,std} + \alpha_{NaOH}\left(T - T_{NaOH,std}\right)}{C_{NaOH,std}} \quad (3)$$

$$\lambda_{NaAc} = \frac{\kappa_{NaAc,std} + \alpha_{NaAc}\left(T - T_{NaAc,std}\right)}{C_{NaAc,std}} \quad (4)$$

With the overall rate of reaction and species concentrations determined, the group was tasked with developing an understanding of the different reactors to successfully obtain the specified products, ethanol and sodium acetate. Therefore, the overall operation and design of the reactor is critical to effectively execute the industrial operations to achieve a high and economical production of the desired products. Today, there are various types of chemical reactors, which can be classified into two main categories: batch and flow reactors.

Varying greatly from a flow reactor, a batch reactor is another type of reactor used in the chemical industrial sector today. Used in a wide variety of applications, a batch reactor has been defined as a closed system that operates under unsteady-state conditions [1]. This means that there are no flows in or out, and the reactor volume is held constant. Normally, batch reactors produce high conversion rates and small amounts of products, but require a relatively long reaction time and mainly deal with liquid phase reactions.

In this portion of the saponification experiment, the group measured the experimental variables of temperature, time, and conductivity to determine the dependence of conversion versus time, equilibrium conversion, reaction rate coefficient, and productivity. To obtain an estimate of the activation energy for the saponification reaction, the linearized Arrhenius equation was used to produce a graph of $\ln(k)$ vs. $\frac{1}{T}$. The group then recorded the estimated activation energy from the developed Arrhenius equation to compare to literature values and the values obtained by the PFR and CSTR reactor systems.

Two main categories of ideal flow reactors operated in the chemical industrial sector under steady-state conditions are plug flow reactors (PFRs) and continuous stirred tank reactors (CSTRs). PFRs are operated at steady-state, where feed is introduced at one end of the cylindrical tube and can flow continuously through the entire length of the reactor. Thus, at the inlet, the reactant concentration is very high; hence, the rate of reaction also high. When it

passes through the reactor, the rate of reaction drops with respect to the reactor length as reactants are consumed and products are formed.

The main advantages of a PFR are that they can run for greater lengths of time with minimal maintenance and have high volumetric reaction conversion due to the lower yield of undesired product. Additionally, when the PFR reaction is larger than zeroth order, the PFR volume will be lower the CSTR volume for the same conversion and reaction conditions. From the industrial production point of view, a PFR can be arranged as a single tube or in the form of a coil contingent on the process application. PFRs are extensively employed in the chemical process industry for both liquid and gas phase reactions.

For the PFR reaction of the saponification experiment, the group measured the experimental variables of time, conductivity, and temperature to determine the dependence of steady- state conversion, equilibrium conversation, reaction rate coefficient, and productivity on varying reaction temperatures and residence times. Since the properties of the flowing stream vary from one point to another, specific assumptions are made about the extent of mixing. The ideal PFR is run at steady-state, constant density, constant tube diameter, and equimolar initial concentrations of sodium hydroxide and ethyl acetate. From there, the saponification's second order reaction rate was integrated to estimate the reaction rate coefficient. Since temperature was varied, the linearized Arrhenius equation provided a graph of $\ln(k)$ vs. $\frac{1}{T}$ that allowed the group to record the estimated activation energy from the slope to compare to literature values and the values obtained by the batch and CSTR reactor systems.

The other flow reactor used in this saponification reaction is a CSTR, where reactants are fed in at a controlled rate and reacted product is continuously drawn off. The outlet streams from the CSTR have the same concentrations as the reaction mixture within the reactor. The CSTR is the idealized opposite of the well-stirred batch and tubular PFRs.

Since the compositions of mixtures leaving a CSTR are at operating concentrations, the reaction driving forces are inevitably low. Therefore, a CSTR requires the largest volume, except for zeroth and negative order, to obtain the preferred conversions. However, the small

driving force allows for better control of both rapid exothermic and endothermic reactions. When high conversions of reactants are needed, several CSTRs in series can be used.

CSTRs in series are simpler and easier to design for isothermal operation. The reactions that benefit from series arrangements are those with narrow operating temperature ranges, or those requiring close control of reactant concentrations for optimum selectivity. For this saponification reaction, old and new CSTRs were used. Compared to the old CSTR, the new CSTR has a single CSTR and two CSTRs connected in series, where the old CSTR only has a single CSTR. Additionally, the old CSTR varied both the flow rates and temperatures, while the new CSTR was held constant at room temperature, and flow rates were varied. However, the flow rate change still affects the residence time and conversion, which can be analytically determined by measuring the conductivity of ions in the CSTR.

For this part of the saponification experiment, the group measured the experimental variables of the total volumetric feed rate, time, conductivity, and temperature. These values were then used to evaluate the steady-state conversion, reaction rate coefficient, and productivity for both the old and new CSTR. To simplify the model material balance equation, specific assumptions were identified. These assumptions included that the reactor was run at steady-state, that the equimolar concentrations of both sodium hydroxide and ethyl acetate were introduced, and that there was perfect mixing. To obtain the estimate of the activation energy for the saponification reaction, the linearized Arrhenius equation was used to produce a graph of $\ln(k)$ vs. $\frac{1}{T}$. The estimated activation energy was compared to literature values and the values obtained by the PFR and batch reactor systems.

Overall, in this saponification experiment, the group simulated the saponification of ethyl acetate in the presence of a strong base, sodium hydroxide, by varying the reactor temperature and reactant flow rates. These results improve the understanding of reaction kinetics regarding the saponification reaction and are very useful in the design of individual reactor systems used in the industrial sector today. For this specific saponification experiment, fractional conversions of the reaction were determined using the conductivity values of the reactants and products under different temperatures. Additionally, the estimated activation energy was

observed from the slope of the graph of $\ln(k)$ vs. $\frac{1}{T}$. Thus, to validate the specific experimental variables for each reactor, the resulting estimated activation energies were compared with both literature values and the values obtained by the other reactor systems.

2.0 Experimental Methodology

2.1 Equipment and Apparatus

There were three batch reactor units used during this experiment: one that was run at room temperature, one at 35ºC, and one at 45ºC. The batch reactor unit shown in Figure 2 was run at 35ºC.

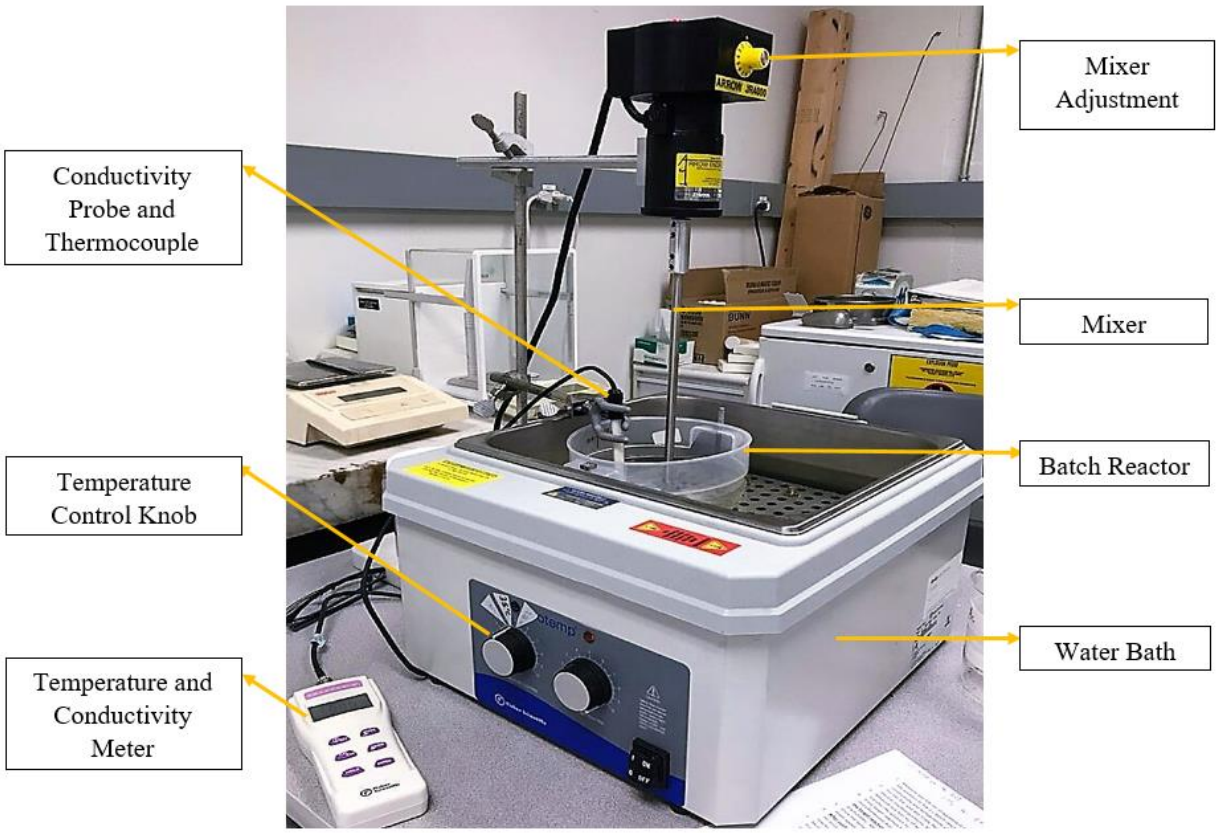


Fig. 2. Batch Reactor unit used in the experiment with hot plate.

The unit was composed of a 2-liter batch reactor located in a water bath in which the temperature was set by the temperature control knob. The reactants consisted of 500 mL of 0.1M NaOH and 500 mL of 0.1M ethyl acetate. Both reactants were heated simultaneously but separately until they stabilized at the target reaction temperature. Once the two reactants

reached the target temperature, they were added together in the batch reactor and the mixer was set to 1 on its dial for the remainder of the reaction.

To record the progress of the reaction, the temperature and conductivity were measured every 10 seconds for the first 3 minutes of the reaction by a digital thermocouple and conductivity meter probe placed in the reaction solution. After the initial 3 minutes, the conductivity and temperature were measured every 20 seconds until the change in conductivity was less than 0.04 mS over a three-minute interval. The reaction was then allowed to reach equilibrium when the product could be extracted from the batch reactor.

The old CSTR configuration in Figure 3 featured a 1.67 L reactor that was fed reactants from two feed tanks via pumps at room temperature. One feed tank held a 0.1M solution of NaOH while the other contained a 0.1M solution of ethyl acetate. The pumps were both set at a volumetric feed rate of 50 mL/min for trial 1, 70 mL/min for trial 2, and 30 mL/min for trial 3. A mixer was used inside the CSTR and dialed to 150 RPM to ensure proper mixing of the reactants. Like the batch reactor, the temperature and conductivity were recorded in the LabView program to track the progress of the reaction.

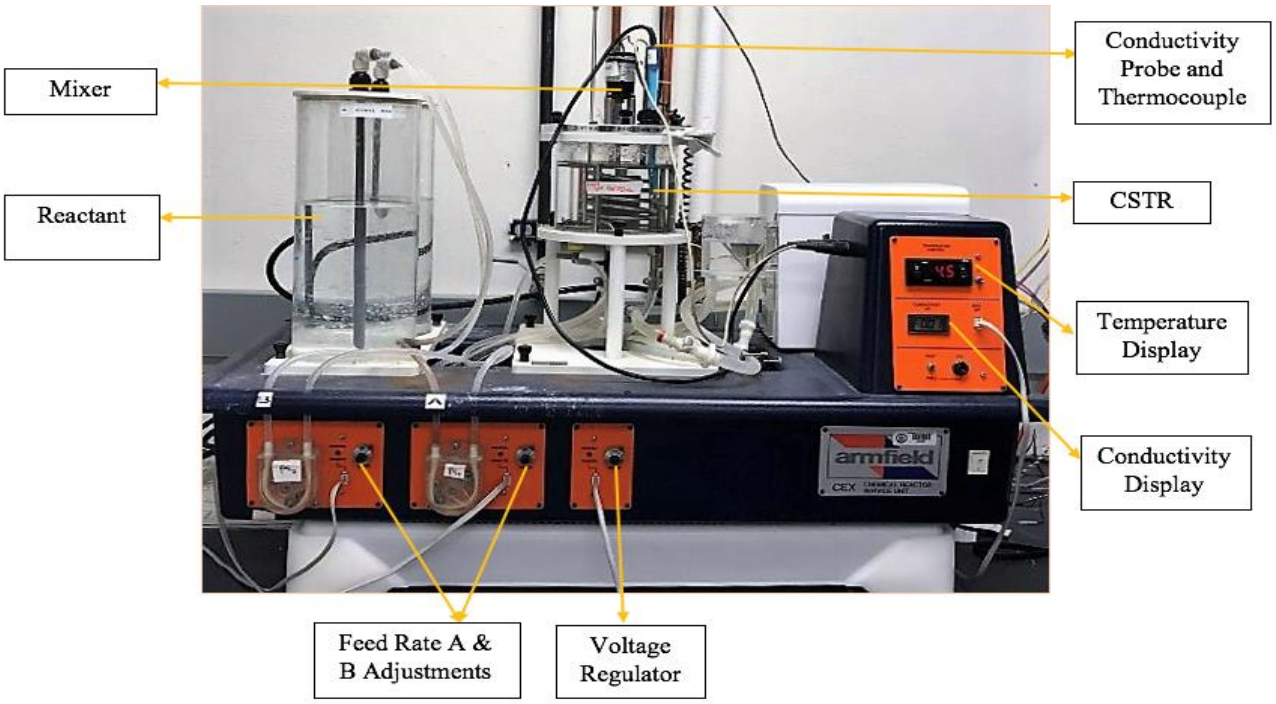


Fig. 3. Old CSTR unit used in the experiment.

Once the CSTR reached steady-state at room temperature (when change in conductivity was less than 0.05 mS over a three-minute interval), data was recorded by LabView for 10 minutes. After the 10 minutes, the reaction temperature was increased to 35ºC and the system was allowed to reach steady-state. When steady-state was reached, data was recorded for 10 minutes. The CSTR was then increased to 45ºC and steady-state was achieved once more. At steady-state, data was recorded for another 10 minutes. The final product from the reactor was continuously discharged throughout the experiment, as it is a continuous process.

The new CSTR system in Figure 4 included both an 800 mL single CSTR and two 400 mL CSTRs in series. Both reactor systems were fed reactants from two feed tanks via pumps at room temperature. Like the old CSTR setup, one feed tank held a 0.1M solution of NaOH and the other contained a 0.1M solution of ethyl acetate. Both pumps circulated the reactants at a 40% capacity setting. The rotameters were used to dial in the reactant flows. For trials 1, 2, and 3, the flow rate for each reactant was set at 76 mL/min, 31 mL/min, and 51 mL/min, respectively.

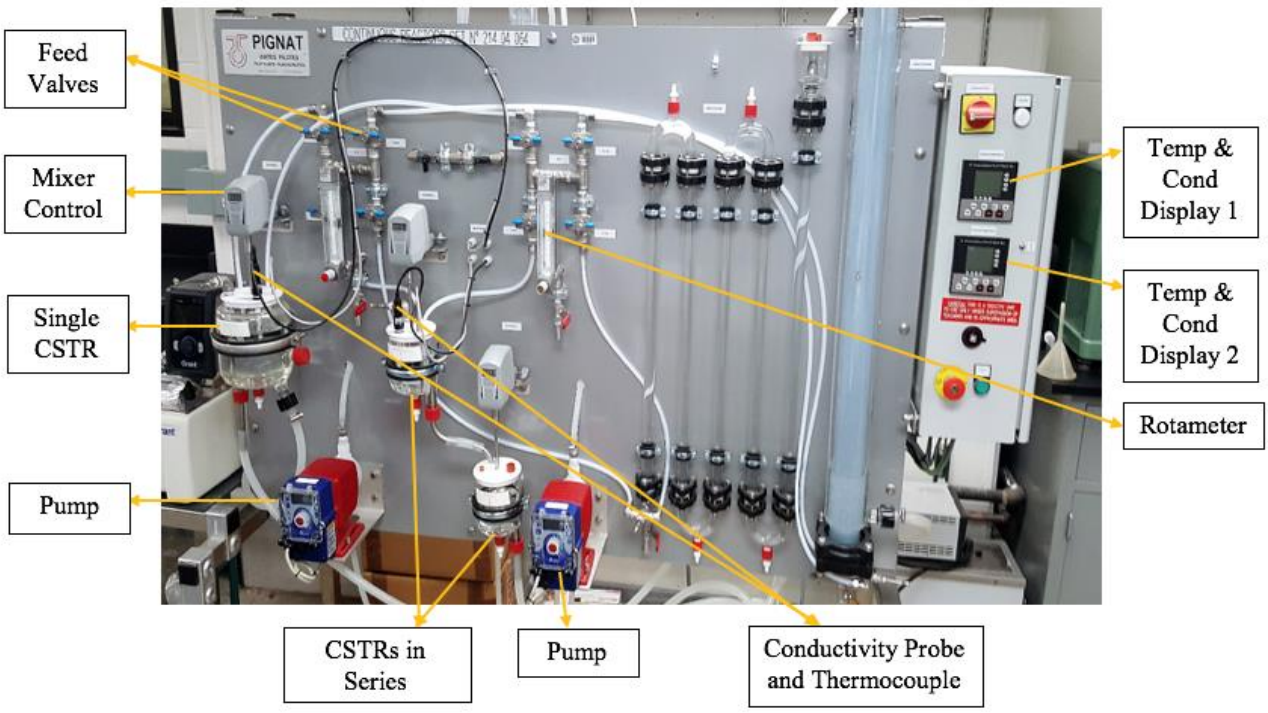


Fig. 4. New CSTR unit used in the experiment.

For the single 800 mL CSTR the mixer was set at 650 RPM. The reactant feed valves for the large CSTR were opened, and once the reactant flows were steady, the temperature and conductivity were recorded every minute from digital display two on the CSTR system. The temperature and conductivity were recorded until the CSTR reached steady-state (when change in conductivity was less than 0.04 mS over a three-minute interval). The conductivity probe and thermocouple were moved from the single CSTR to the second CSTR in the CSTR cascade.

The mixers for the 400 mL CSTRs in series were set at 375 RPM. The reactant feed valves for the CSTR cascade were opened, and once the flow rates were steady, the temperature and conductivity were recorded every minute from digital display one on the CSTR system. The temperature and conductivity were recorded until the second CSTR in the CSTR cascade reached steady-state (when change in conductivity was less than 0.04 mS over a three-minute interval). Once the second reactor reached steady-state, the conductivity probe and thermocouple were moved to the first reactor in the series to verify that the first CSTR was at steady-state as well.

The PFR unit (shown in Figure 5) employed a 1 L tubular reaction chamber which was fed reactants from feed tanks via pumps. A 0.1M solution of NaOH and a 0.1M solution of ethyl acetate were the reactants fed by the pumps. The reactant flow rates for trials 1, 2, and 3, were dialed to their respective flow rates of 130 mL/min, 100 mL/min, and 80 mL/min, by a rotameter.

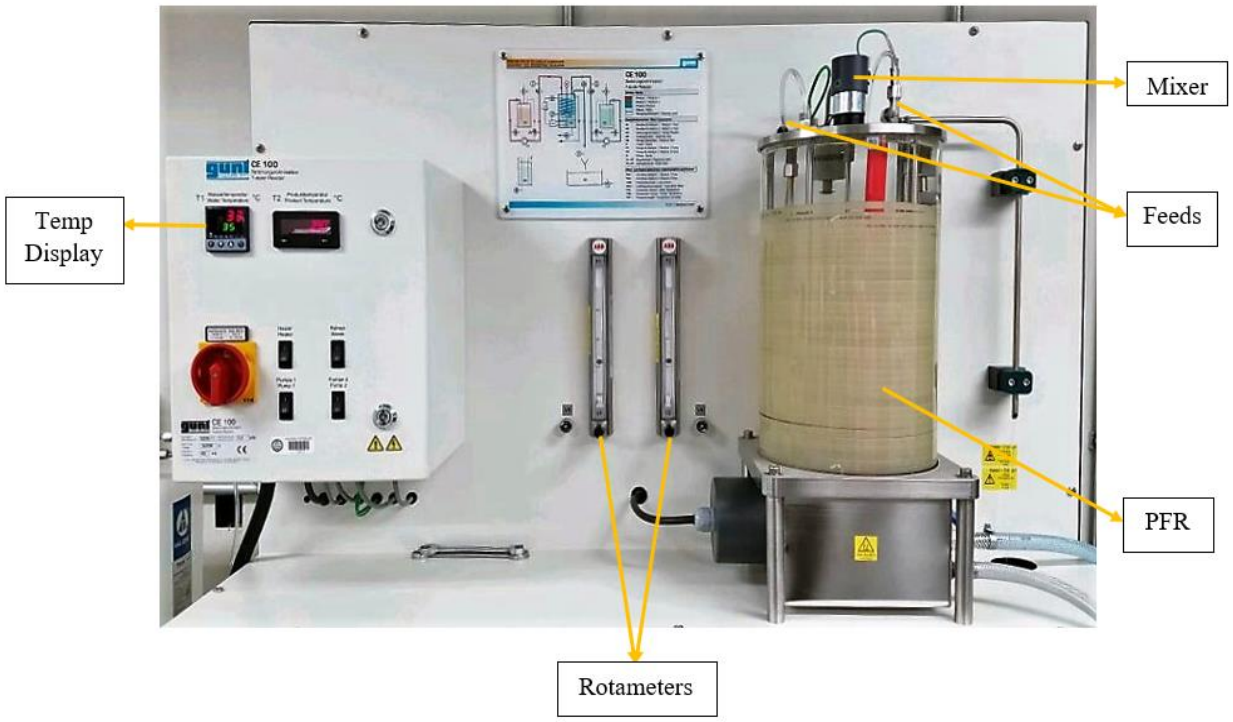


Fig. 5. PFR unit used in the experiment.

Once the reactant flow rates were steady, a product sample at room temperature was taken every minute, and its conductivity was measured using a hand-held probe. The reactor temperature was recorded from the reactor panel. Data was recorded for 20 minutes when steady-state was determined to be reached. Once steady-state was reached at room temperature, the reactor chamber temperature was increased to 35ºC. The same procedure that was run at room temperature was also run at 35ºC and 45ºC.

2.2 Experimental Variables and Key Measures

In all three batch reactor experiments, the experimental variable investigated was temperature. The reaction temperature was controlled by a water bath. The data compiled from the three different trial temperatures enabled the effect of temperature on reaction rate to be investigated. Other variables such as mixing speed, feed rate, reactor volume, and reactant concentrations were held constant in all of the trials so that temperature was the only variable changing. Key measurements taken from each batch trial included conductivity, temperature, and time.

The experimental variables investigated during the old CSTR experiment included temperature and residence time. Three trials were run on the old CSTR. Trial 1 had both reactant feed rates at 50 mL/min, trial 2 was at 70 mL/min, and trial 3 was at 30 mL/min. During each trial, data was taken after steady-state was reached at room temperature, 35ºC, and 45ºC. Key measurements from each old CSTR trial included: conductivity, temperature, and time. From the data recorded, the effects of temperature and residence time on reaction rate and productivity can be determined. Other variables held constant were reactor volume, mixing speed, and reactant concentrations.

During the new CSTR experiment, the experimental variables investigated included residence time and reactors in series. Three trials were run on the new CSTR. Trial 1 had both reactant feed rates at 76 mL/min, trial 2 was at 31 mL/min, and trial 3 was at 51 mL/min. During each trial, data was taken until steady-state was reached on the single 800 mL CSTR. Once the single CSTR reached steady-state, reactants were then fed to two, 400 mL CSTRs in series until they reached steady-state. Key measurements from each new CSTR trial included conductivity, temperature, and time. From the data, the effect on conversion, productivity, and residence time can be determined from reactant flow rates and reactor cascades. Other variables held constant were temperature, mixing speed, and reactant concentrations.

In the PFR trials, the experimental variables investigated were temperature and reactant feed rate. Three trials were run on the PFR, trial 1 had a reactant feed rate of 130 mL/min, trial 2 was 100 mL/min, and trial 3 was 80 mL/min. During each trial, data was taken until steady-state was reached at room temperature, 35ºC, and 45ºC. Key measurements from each PFR

trial included conductivity, temperature, and time. With the data recorded, the effects of temperature and residence time on reaction rate coefficient, conversion, and productivity in a PFR can be determined. Other variables held constant during the experiment were reactor volume, mixing speed, and reactant concentrations.

3.0 Results

3.1 Thermodynamic Analysis

The heat of reaction and the standard Gibbs free energy change of reaction were found using literature formation values. The estimated values are given in Table 1.

Table 1. Estimation of Thermodynamic Values for the Saponification Reaction

Thermodynamic Value	Value (kJ/mol)
Heat of Reaction (ΔH_R)	-81.0
Standard Gibbs Free Energy Change of Reaction (ΔG_R)	-68.4

The equilibrium constant (K_{eq}) was found using the standard Gibbs free energy change of reaction and the respective batch temperature. These values were then used to find the equilibrium conversion of NaOH for the reaction at each temperature. These values are given in Table 2.

Table 2. Equilibrium Values for Saponification

Thermodynamics	Room Temp (22°C)	35°C	45°C
K_{eq} ($*10^{11}$)	12.9357	3.98639	1.721
X_{eq}	0.999999121	0.999998416	0.999997589

3.2 Batch Reactor

For the batch reactor, experimental data was used to examine the dependence of conversion versus time for each reaction temperature (room temperature, 35ºC, 45ºC). Equilibrium conversion, reaction rate coefficient, and productivity were also determined at each reaction temperature investigated. The activation energy of the reaction was calculated using the reaction rate coefficients. Each of these variables was evaluated twice for each experimental session thus far.

Figures 6, 7, and 8 show the conversion profiles of the saponification reaction at each batch temperature for sessions one through three, respectively.

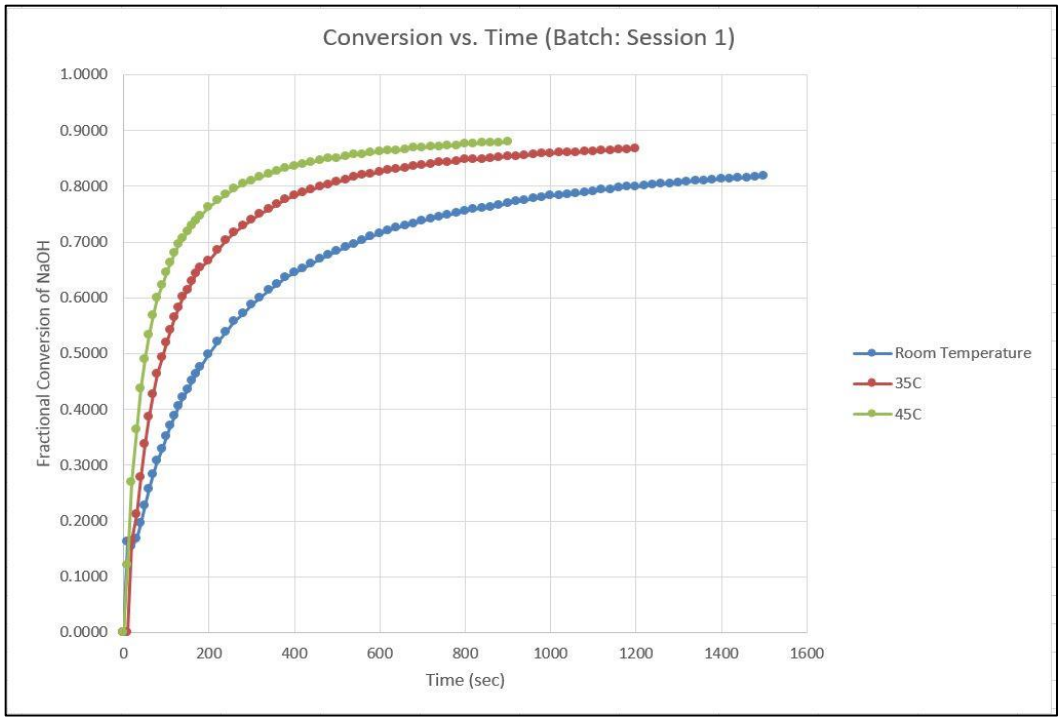


Fig. 6. Conversion Profiles for the Batch Reactor (Session 1)

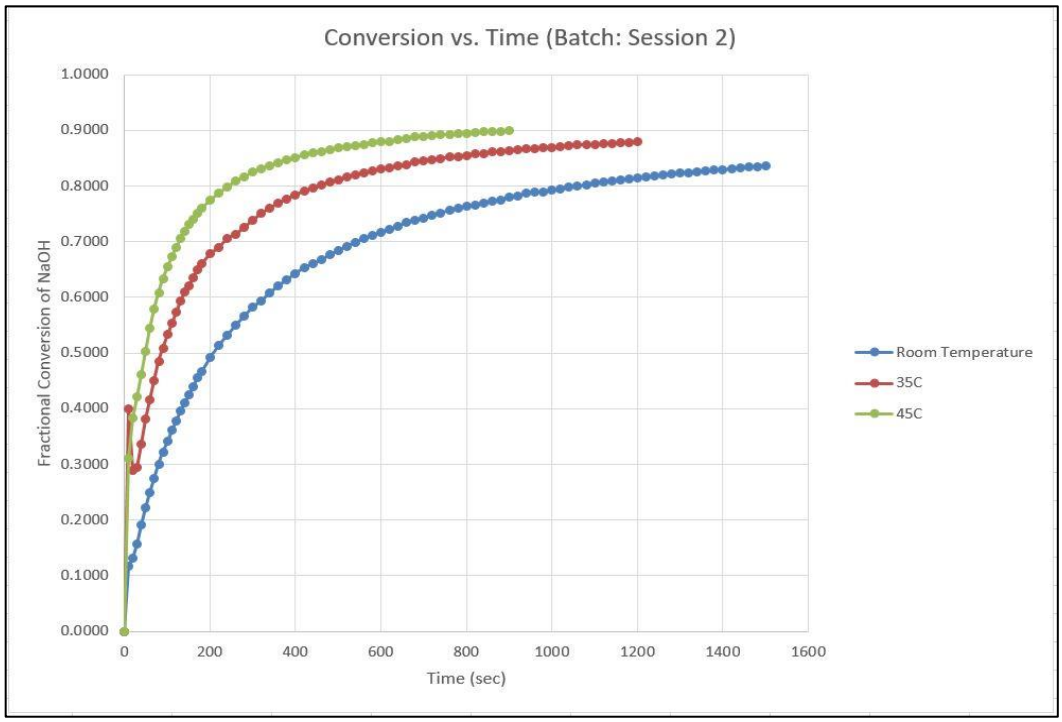


Fig. 7. Conversion Profiles for the Batch Reactor (Session 2)

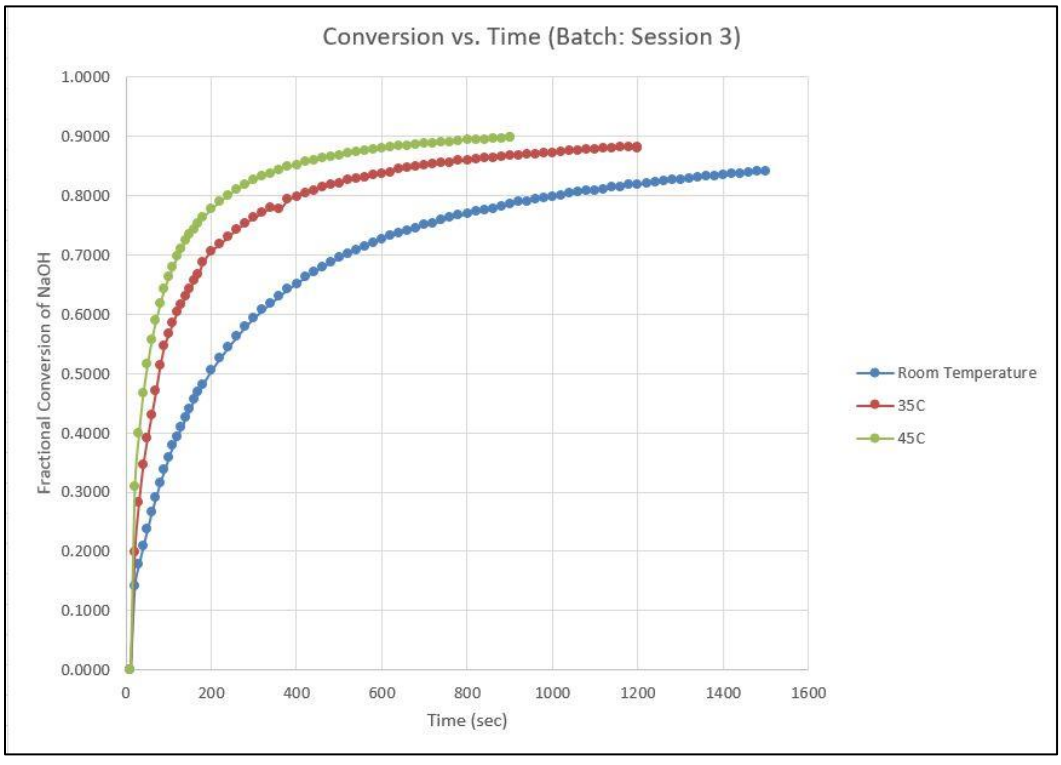


Fig. 8. Conversion Profiles for the Batch Reactor (Session 3)

Table 3 shows the rate coefficients for each temperature for both experimental sessions.

Table 3. Reaction Rate Coefficient at each Batch Temperature

k (L/mol*s)	Room Temp (22°C)	35°C	45°C
Session 1	0.0939	0.2177	0.3300
Session 2	0.0926	0.1938	0.3341
Session 3	0.0997	0.2417	0.3550

Graphically, the activation energy could be found by plotting the natural log of the reaction rate against the inverse of each respective temperature (in Kelvin). Figures 9, 10, and 11 show the plots used to find activation energy for each session.

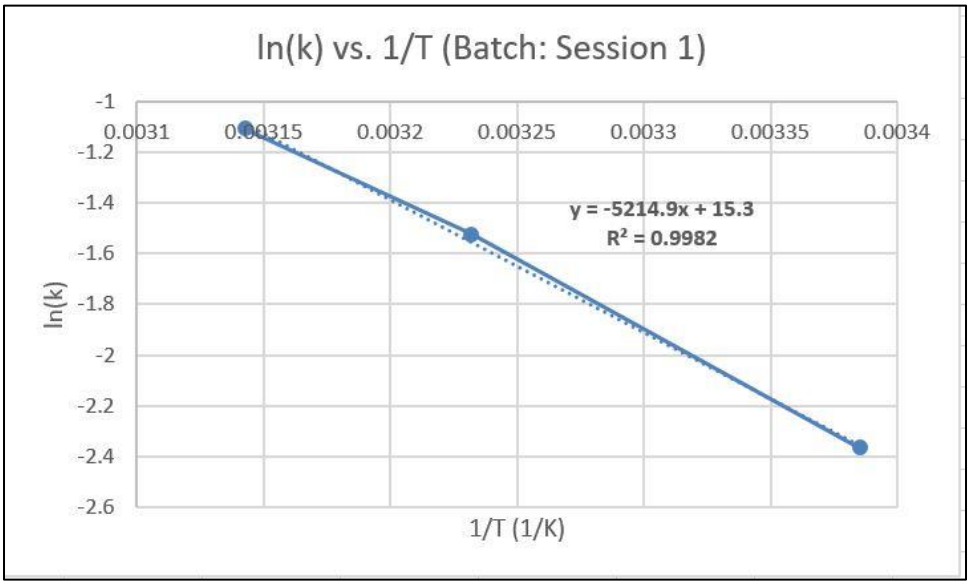


Fig. 9. Plot used to find Activation Energy (Session 1)

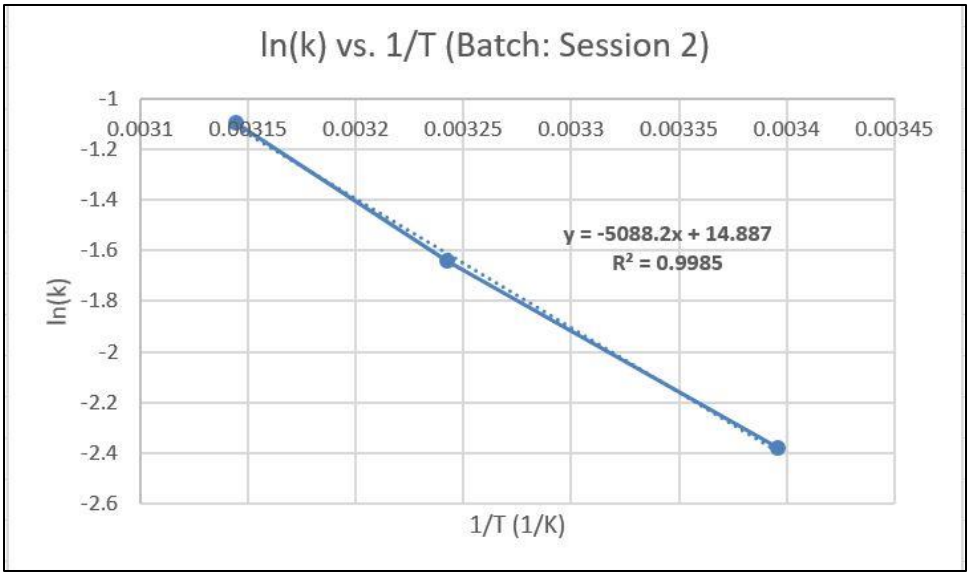


Fig. 10. Plot used to find Activation Energy (Session 2)

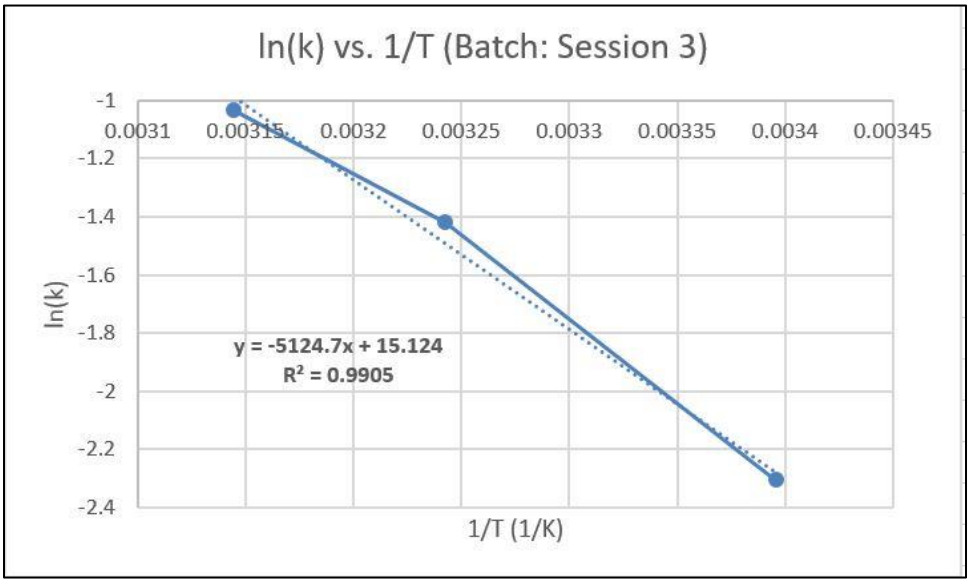


Fig. 11. Plot used to find Activation Energy (Session 3)

The activation energy was found by multiplying the slope by the negative ideal gas constant (R = 8.314 J/mol*K). The activation energies that were found from each experimental session as well as the literature value are given in Table 4.

Table 4. Activation Energy Calculations

	Activation Energy (kJ/mol)
Session 1	43.357
Session 2	42.303
Session 3	42.608
Literature Value	41.4

Productivity calculations were based on a conversion of about 60%. Figures 12, 13, and 14 show plots of the reaction productivity at each batch temperature for each session.

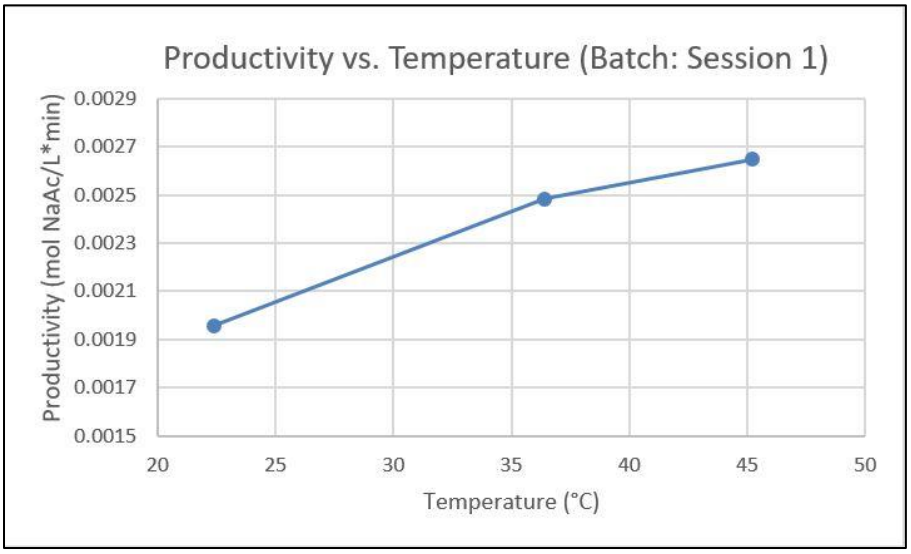


Fig. 12. Productivity versus Batch Temperature (Session 1)

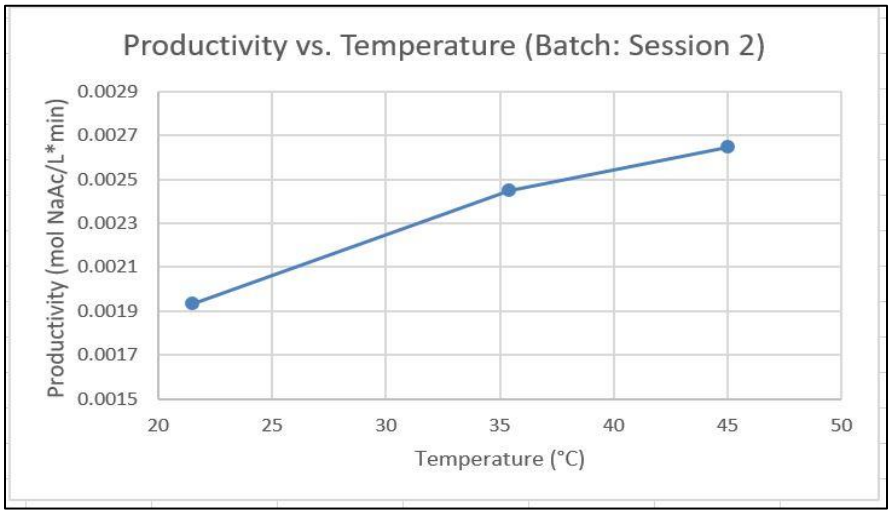


Fig. 13. Productivity versus Batch Temperature (Session 2)

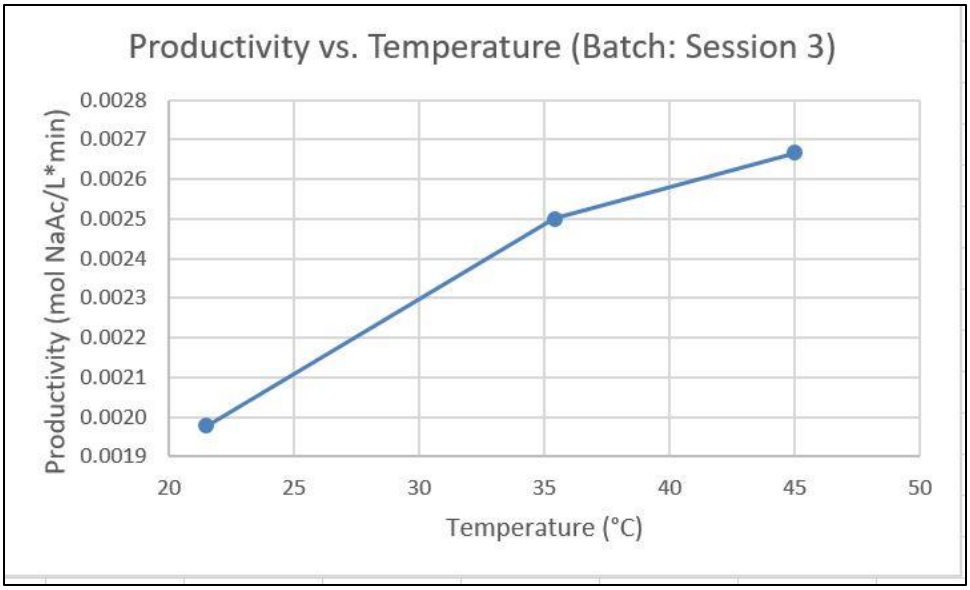


Fig. 14. Productivity versus Batch Temperature (Session 3)

3.3 Old CSTR

The next reactor investigated was the old CSTR. For the first experimental session, the flow rates of both the NaOH and ethyl acetate were maintained at 50 mL/min, and the conductivity of the solution at steady-state was recorded at three different temperatures: room temperature (~25°C), 35°C, and 45°C. The same procedure took place for the second and third experimental sessions except that the flow rates of the NaOH and ethyl acetate were increased to 70 mL/min and decreased to 30 mL/min for each temperature, respectively. With a CSTR volume of 1.67 L, Figure 15 shows how residence time was affected by the flow rate.

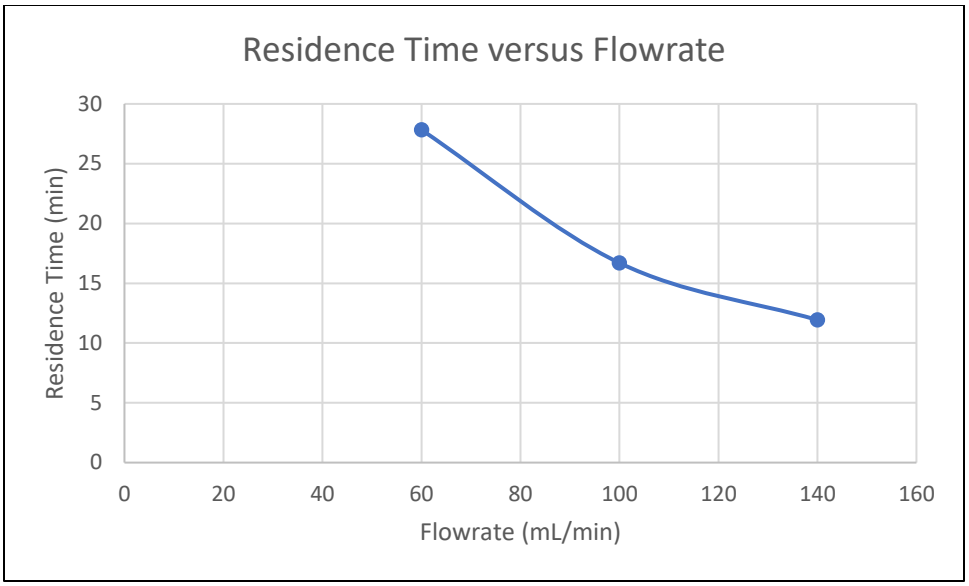


Fig. 15. Residence time versus the flow rate for each experimental session.

The first technical objective of this reactor was to understand how steady-state conversion depends on the reaction temperature and residence time. Using the data from experimental session one, the reactor running at room temperature, and Equations 3 and 4, the specific conductance of NaOH and NaAc was calculated, and the average was used since ten steady-state data points were recorded. Once the specific conductance was calculated, the percent conversion was found and averaged. The same calculations were also made for the reactor temperatures of 35°C, and 45°C, and repeated for experimental session 2 and 3 at each of the respective flow rates. Figure 16 shows the reactor temperature versus conversion while Figure 17 shows the residence time versus conversion. These graphs show that conversion increases with both temperature and residence time.

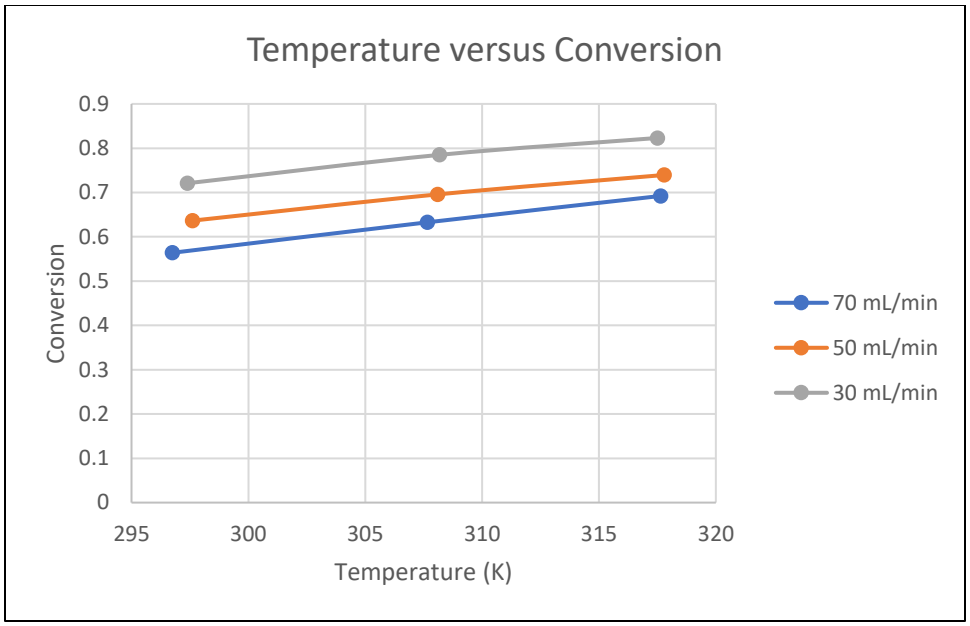


Fig. 16. Conversion versus reactor temperature for both experimental sessions.

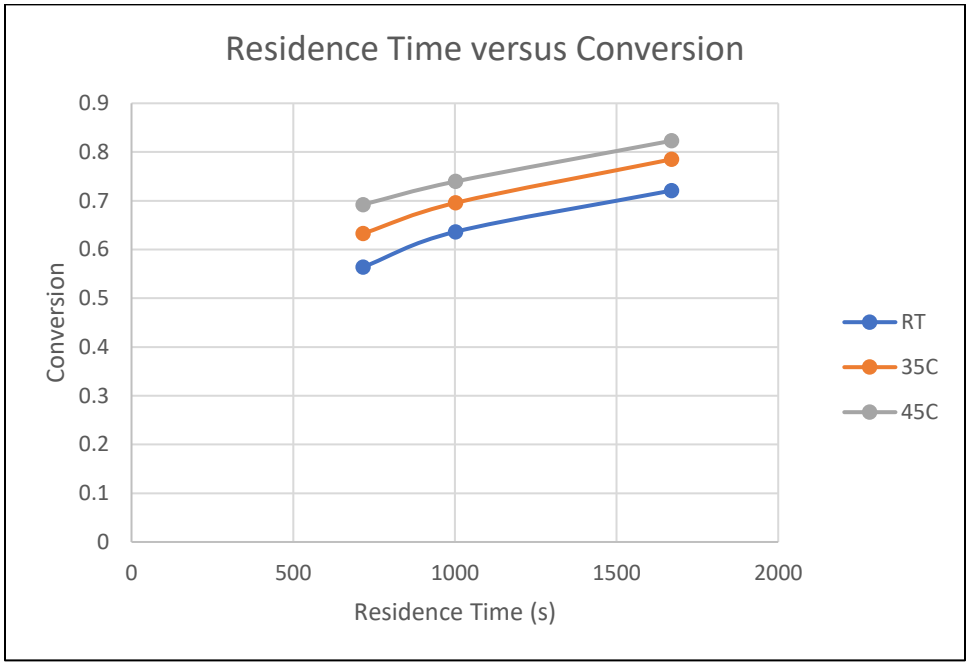


Fig. 17. Conversion versus residence time for both experimental sessions.

Using Equation 20 in Appendix 2, the rate constants at each temperature and for both experimental sessions were calculated. Table 5 shows the calculated rate constants.

Table 5. Rate constants in units of L/(mol*s) for temperatures at each flow rate.

Temperature	**τ = 27.83 min**	**τ = 16.70 min**	**τ = 11.93 min**
Room Temperature	0.1108	0.0961	0.0829
35°C	0.2033	0.1500	0.1310
45°C	0.3149	0.2177	0.2042

To solve for the activation energies of each flow rate, a plot of 1/T versus the natural log of the respective rate constant was plotted. The slope of this line was equivalent to -Ea/R, in which case the activation energy was found. Table 6 shows the activation energies for both residence times. The calculated activation energies are similar to each other for the shorter residence times but much less than the literature value of the saponification reaction. However, the activation energy of the residence time of 27.83 minutes is very close to that of the literature value.

Table 6. Activation energy for each residence time.

	Activation Energy (kJ/mol)
τ = 27.83 min	40.87
τ = 16.70 min	31.86
τ = 11.93 min	33.79
Literature Value	41.4

To solve for the productivity for each temperature at each residence time, Equation 22 in Appendix 2 was used. Figure 18 shows the productivity of NaAc versus temperature and Figure 19 shows the productivity of NaAc versus residence time. The productivity increased as the temperature increased and the residence time decreased.

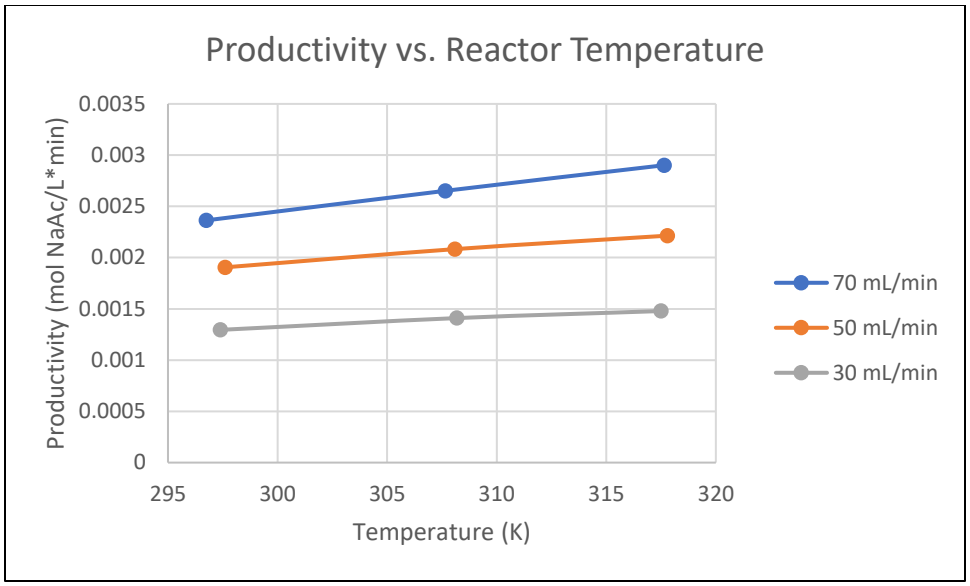


Fig. 18. Productivity vs reactor temperature

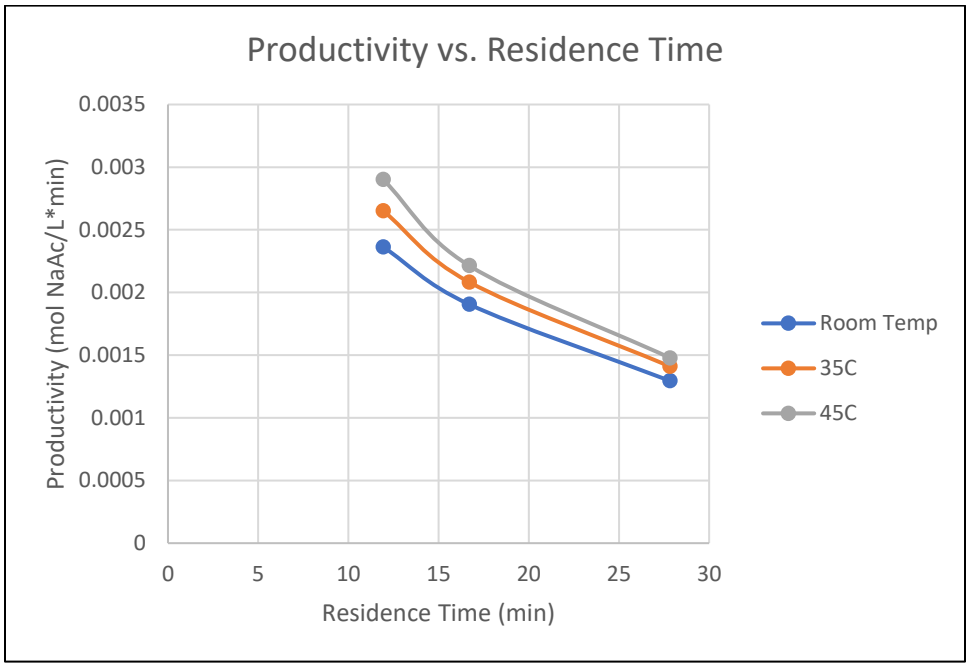


Fig. 19. Productivity vs residence time

3.4 New CSTR

In completing the technical objective for the New CSTR, conversion, residence time, and productivity were calculated from experimental data for a single CSTR and two CSTRs in series. Data was collected at room temperature and at three different volumetric flow rates, 62 mL/min, 102 mL/min, and 152 mL/min. As observed in Table 7, the overall conversion at each

volumetric flow rate was higher for a series of two CSTRs than for a single CSTR. It was also observed that at 62 mL/min, the conversions for the single and the series configurations were higher than those of the same configurations at 102 mL/min and 152 mL/min.

Table 7. New CSTR Overall Conversions

CSTR Configuration	Volumetric Flow Rate (mL/min)	Conversion
Single	62	0.458
Series	62	0.536
Single	102	0.403
Series	102	0.466
Single	152	0.354
Series	152	0.417

The individual conversions for the two reactors in series were also calculated at each volumetric flow rate and are summarized in Table 8. For all three flow rates, the first reactor in the series gave a higher conversion than the second. Although there was some overlap between the conversions, the general trend was that they decreased as volumetric flow rate increased.

Table 8. New CSTR Individual Conversions for Reactors in Series

Reactor in Series	Volumetric Flow Rate (mL/min)	Individual Conversion
1^{st}	62	0.381
2^{nd}	62	0.251
1^{st}	102	0.294
2^{nd}	102	0.243
1^{st}	152	0.264
2^{nd}	152	0.208

The overall residence time was calculated for each volumetric flow rate. For 62 mL/min, 102 mL/min, and 152 mL/min, the residence times were 12.093 min, 7.843 min, and 5.263 min,

respectively. The trend observed between volumetric flow rate and residence time was that as the flow rate increased, the residence time decreased.

When comparing productivity for single and series configurations at the same volumetric flow rate (Table 9), the series configuration had a higher productivity than the single configuration for all three volumetric flow rates. It was also observed that for both configurations the productivity increased as volumetric flow rate increased.

Table 9. New CSTR Overall Productivity Values

CSTR Configuration	Volumetric Flow Rate (mL/min)	Productivity (mol NaAc/L*min)
Single	62	0.00177
Series	62	0.00208
Single	102	0.00257
Series	102	0.00297
Single	152	0.00336
Series	152	0.00397

3.5 PFR

The technical objective for the PFR was to evaluate how reactor temperature and residence time affected steady-state conversion, reaction rate coefficient, and reaction productivity. The PFR experiment was completed for NaOH and ethyl acetate flow rates of 130, 100, and 80 mL/min at three different temperatures: room temperature, 35ºC, and 45ºC. Time, conductivity, and temperature were recorded for each trial. Based on the data collected, figures were constructed to depict the effects temperature and residence time have on specific reaction characteristics.

Figure 20 shows the residence time for each flow rate. Figures 21, 22, and 23 show how steady-state conversion changes with temperature and residence times for flow rates of 80, 100 and 130 mL/min, respectively.

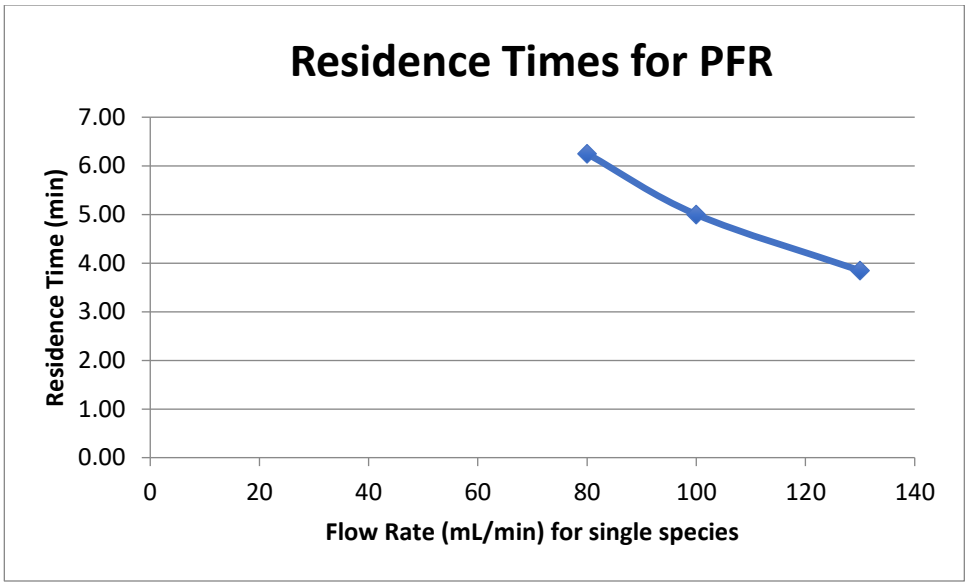


Fig. 20. Plot of residence time versus reactant flow rate

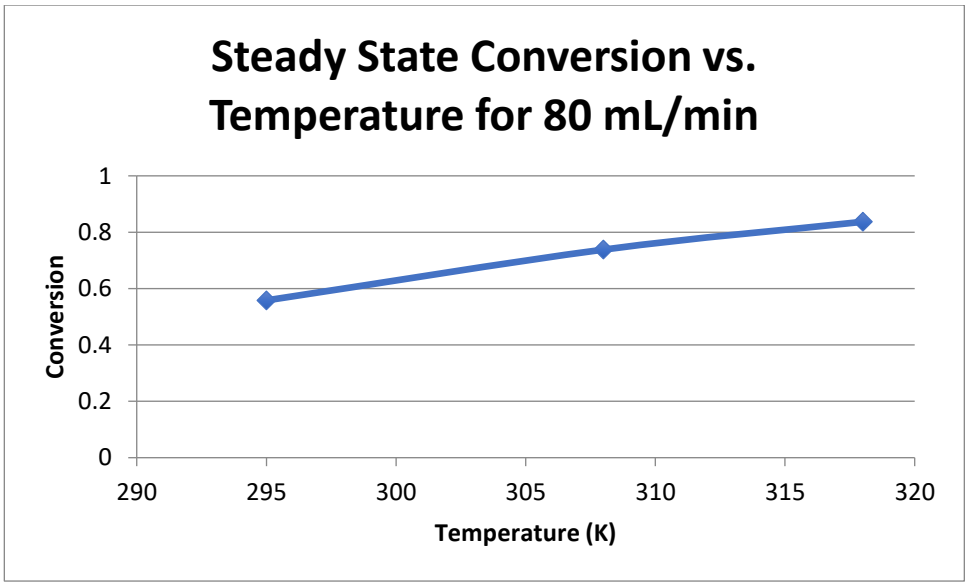


Fig. 21. Plot of steady-state conversion versus temperature for a residence time of 6.25 minutes

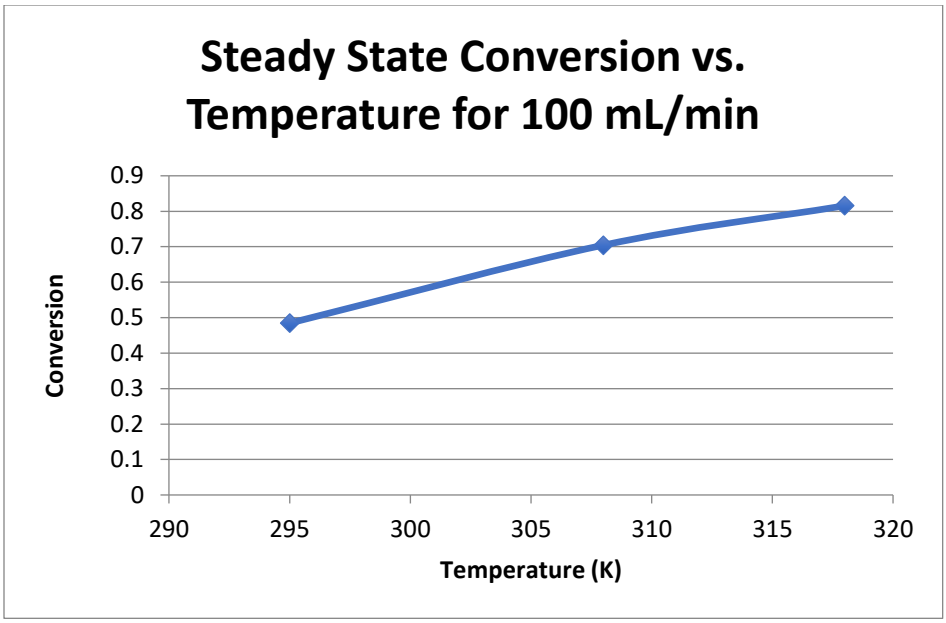


Fig. 22. Plot of steady-state conversion versus temperature for a residence time of 5 minutes

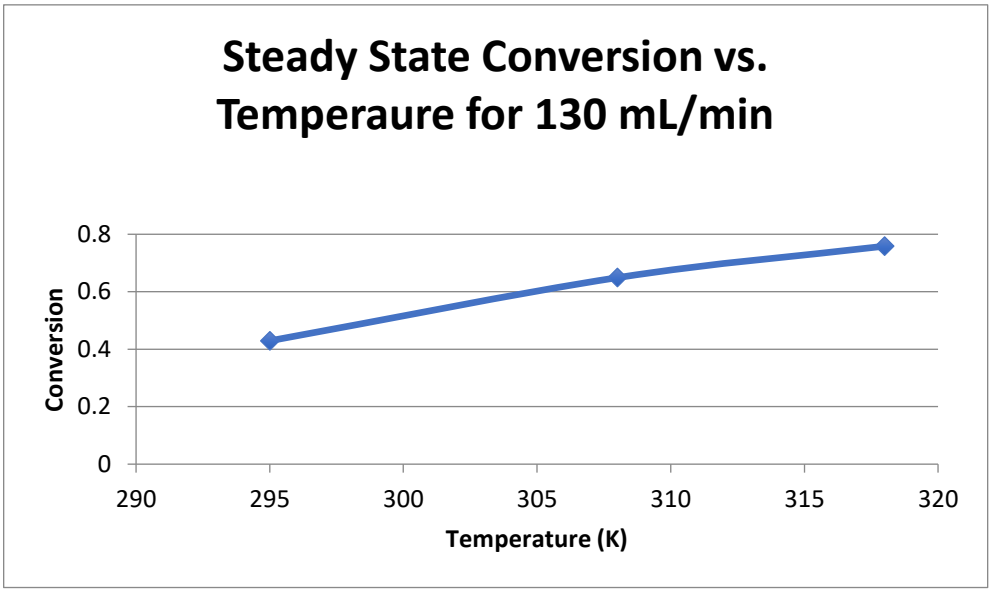


Fig. 23. Plot of steady-state conversion versus temperature for a residence time of 3.85 minutes

To calculate the reaction rate coefficient k for the reactions, the Equation 23 was separated and integrated from 0 to L and $C_{NaOH,o}$ to C_{NaOH} to obtain Equation 24. This was solved for k to evaluate the reaction rate coefficients. Tables 10, 11 and 12 contain the reaction rate coefficients for flow rates of 80, 100, and 130 mL/min, respectively.

Table 10. Reaction rate coefficient k for 80 mL/min flow rate

Temperature (K)	Average S.S. k value (L/mol*sec)
295	0.06738
308	0.15052
318	0.27411

Table 11. Reaction rate coefficient k for 100 mL/min flow rate

Temperature (K)	Average S.S. k value (L/mol*sec)
295	0.06265
308	0.15889
318	0.29489

Table 12. Reaction rate coefficient k for 130 mL/min flow rate

Temperature (K)	Average S.S. k value (L/mol*sec)
295	0.06515
308	0.16021
318	0.27225

Once k values were obtained, plots of ln(k) vs 1/T were made in order to estimate the activation energy based on the Arrhenius equation at different temperatures. The activation energy was estimated by calculating the slope of the Figures 24, 25, and 26 which is -Ea/R. From here, the activation energy was estimated for all three flow rates and then averaged. Table 13 shows the results.

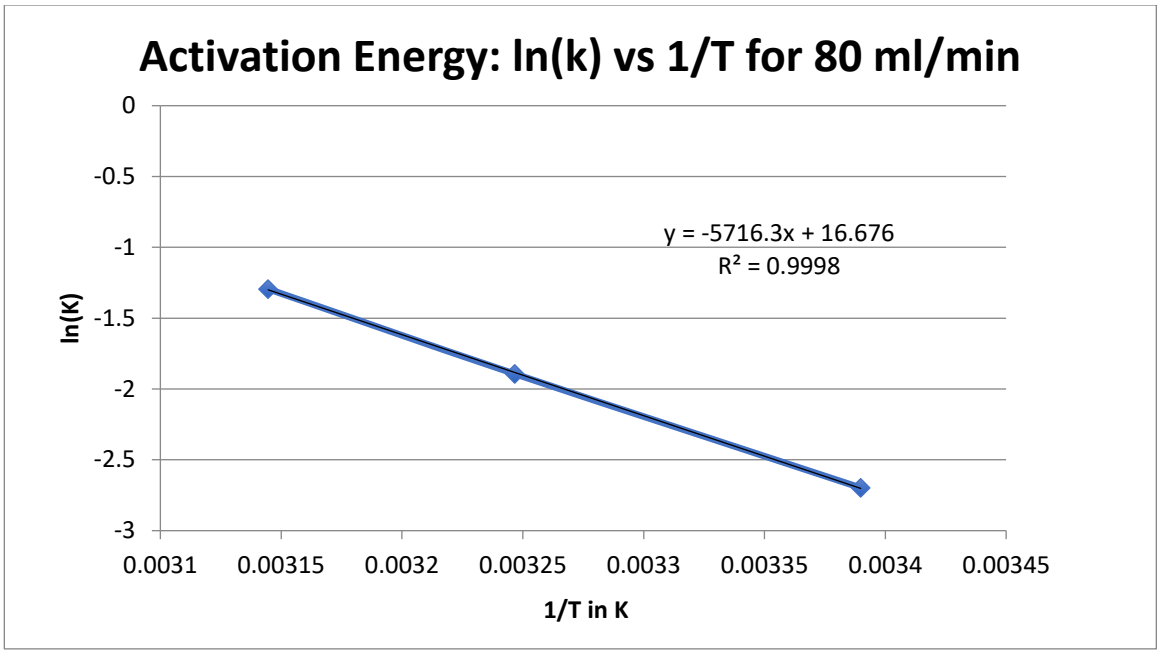


Figure 24. Estimating 80 mL/min activation energy using the slope, -Ea/R

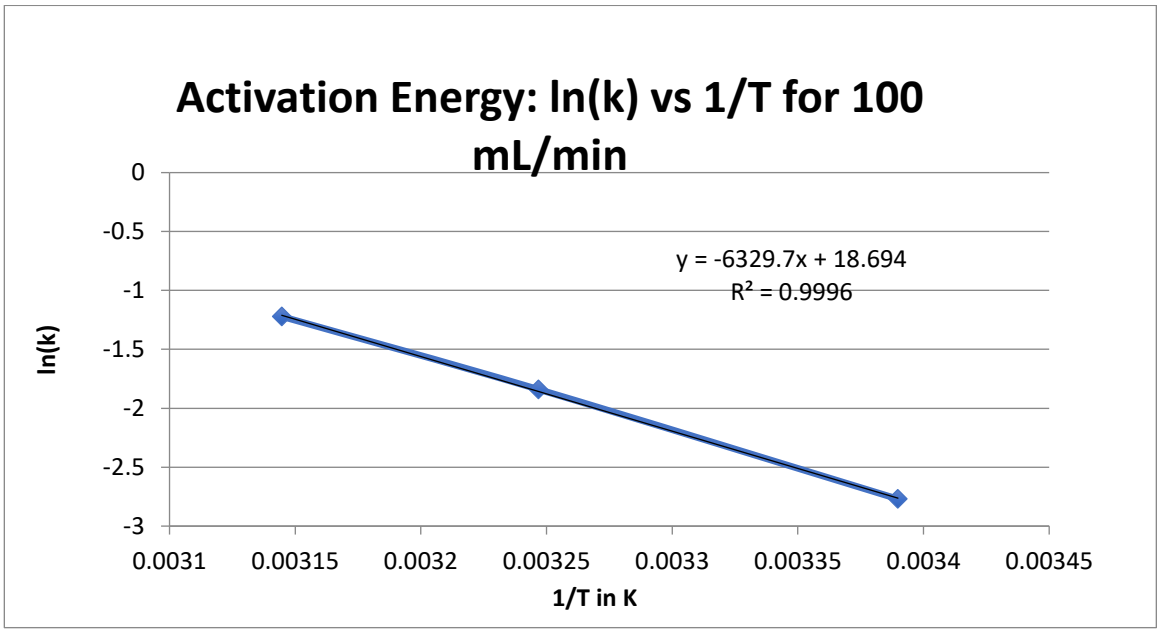


Figure 25. Estimating 100 mL/min activation energy using the slope, -Ea/R

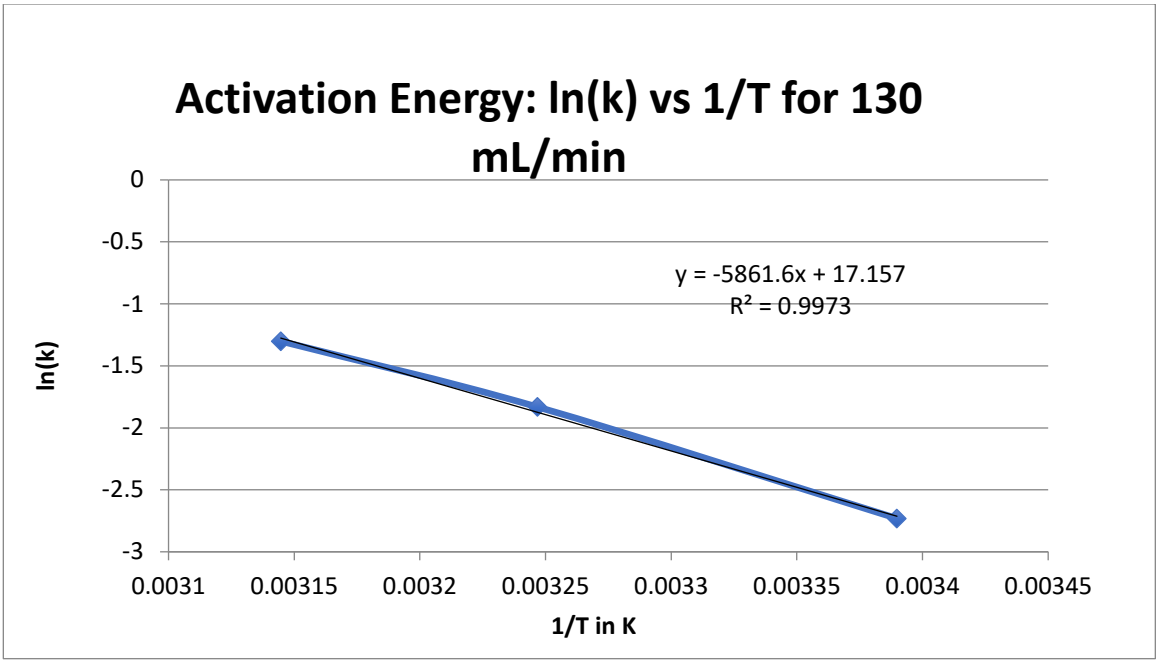


Fig. 26. Estimating 130 mL/min flow activation energy using the slope, -Ea/R

Table 13. Estimated and average activation energies

Activation Energies	
Flow Rate (mL/min)	Activation Energy (kJ/mol)
80 mL/min	47.5 kJ/mol
100 mL/min	52.6 kJ/mol
130 mL/min	48.7 kJ/mol
Average Activation Energy: 49.6 kJ/mol	

After conversion and residence time were calculated, productivity was evaluated using Equation 25 located in Appendix 2. The results are shown in Figures 27, 28, and 29 for all flow rates.

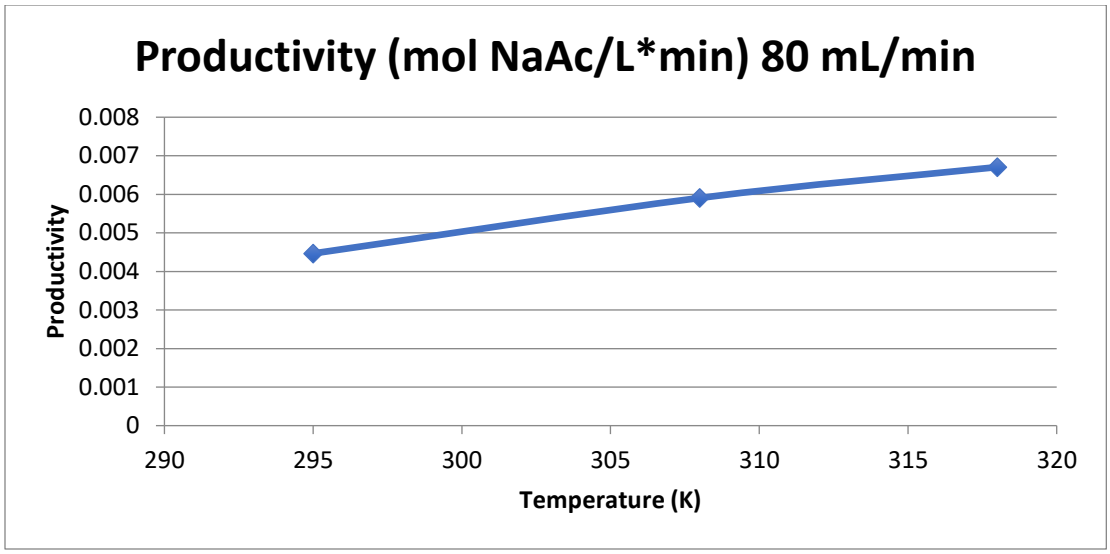


Fig. 27. Productivity versus temperature for 80 mL/min flow rate

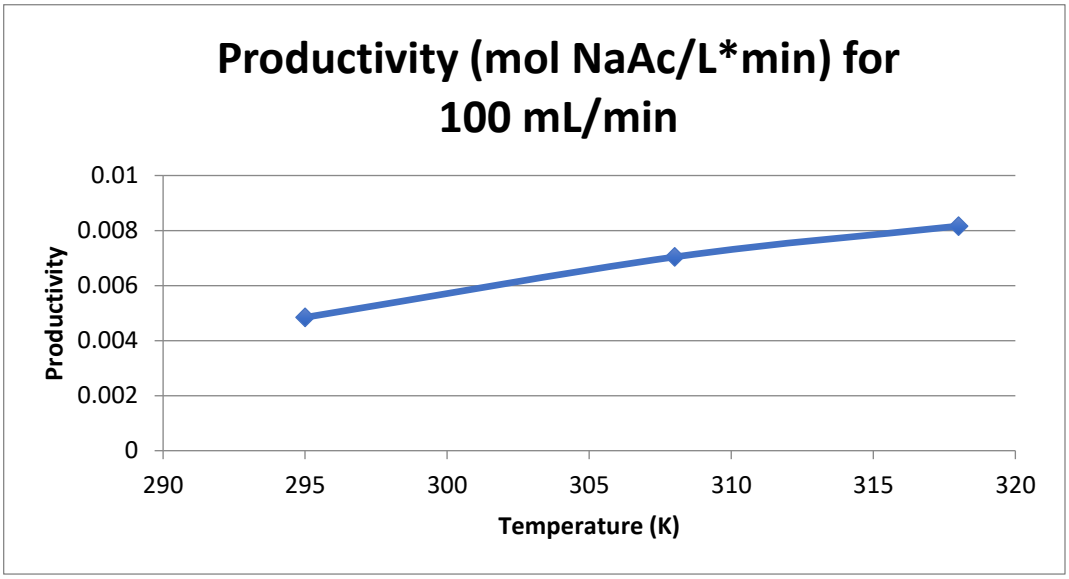


Fig. 28. Productivity versus temperature for 100 mL/min flow rate

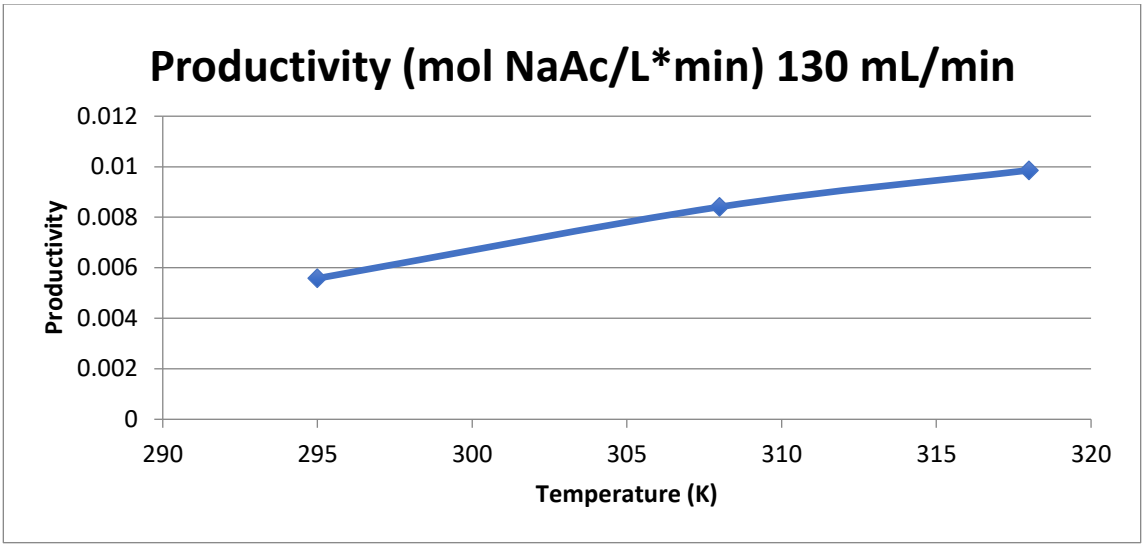


Fig. 29. Productivity versus temperature for 130 mL/min flow rate

Table 14. Statistical Analysis.

	Activation Energy kJ/mol	**k(RTºC) mol NaAc/L*min**	**k(35ºC) mol NaAc/L*min**	**k(45ºC) mol NaAc/L*min**
Batch	43.357	0.0939	0.2177	0.3300
	42.303	0.0926	0.1938	0.3341
	42.608	0.0997	0.2417	0.3550
Old CSTR	40.870	0.1108	0.2033	0.3149
	31.860	0.0961	0.1500	0.2177
	33.790	0.0829	0.1310	0.2042
PFR	47.500	0.0638	0.1505	0.2741
	52.600	0.0627	0.1589	0.2949
	48.700	0.0652	0.1602	0.2723
$\bar{x}$	42.621	0.0853	0.1786	0.2886
s	6.6880	0.0176	0.0370	0.0519
s_x	2.2293	0.0059	0.0123	0.0173
t	2.306	2.306	2.306	2.306
C.I.	42.621 ± 5.1408	0.0853 ± 0.0136	0.1786 ± 0.0284	0.2886 ± 0.0399

4.0 Analysis and Discussion

From the thermodynamic analysis, the heat of reaction was found to be a negative value, -81.0 kJ/mol, meaning that the reaction was exothermic. The standard Gibbs free energy change of reaction was also a negative value, -68.4 kJ/mol, indicating that the reaction was spontaneous. Using Equation 3, K_{eq} could be found at each respective temperature.

Since the reaction was exothermic, running the reaction at higher temperatures should have lowered K_{eq}, due to Le Chatelier's principle. This was verified by the calculations, where K_{eq} and equilibrium conversion decreased as temperature increased. Since K_{eq} was such a large value for each calculation (on the order of 10^{11}), temperature increases had little impact on the equilibrium conversion. Each 10°C increment resulted in a conversion decrease of $7.1*10^{-7}$ and $8.3*10^{-7}$, respectively. As a result, the reverse reaction was assumed to be miniscule compared to the forward reaction, which greatly simplified the calculations for the rest of this report.

Figures 6, 7, and 8 show conversion profiles against time for the batch reactor at each respective temperature. For each experimental session, the 45°C batch reactor showed the fastest conversion time as compared to the other two batch reactors. A conversion of 0.60 was reached at around 320 s at room temperature, around 125 s at 35°C, and around 80 s at 45°C. This made sense, as the higher temperatures increased the rate coefficient due to the Arrhenius equation. This was validated by Table 3, where the rate coefficients increased directly with temperature in both sessions.

The calculated activation energies (43.357 kJ/mol, 42.303 kJ/mol, and 42.607 kJ/mol) in Table 4 were slightly above the literature value of 41.4 kJ/mol. This could be the cause of imperfect reactor conditions such as heat loss due to convection. This would result in values seemingly higher than the literature value, since more energy is used to progress the reaction. However, these values are very close to the literature value, so this error is minor.

Figures 12, 13 and 14 show that the productivity of the batch reactor increased as temperature increased: around 0.00195 mol NaAc/L*min at room temperature, around 0.00250 mol NaAc/L*min at 35°C, and around 0.00265 mol NaAc/L*min at 45°C. Therefore, an optimum running condition for a batch operation for this reaction would be a high-temperature process. This would ensure a shorter residence time, all while keeping a high equilibrium conversion.

The next reactor analyzed was the old CSTR. The reaction inside the old CSTR occurred over the residence time interval. The residence time was found by dividing the volume of the CSTR by the total volumetric flow rate. The three experimental sessions occurred at 60 mL/min, 100 mL/min, 140 mL/min. Based on the equation, the residence time decreased from 27.83 minutes to 16.7 minutes to 11.93 minutes as the total volumetric flow rate increased and can be observed in Figure 15.

In the saponification reaction, both the residence time and the temperature affected the conversion of NaOH. Because of this, both the flow rates and temperatures were altered between the three experimental sessions. For each session, the conductivity was measured when the solution reached steady-state at room temperature, 35°C, and 45°C. Since the reactor was run at outlet conditions, and the concentration was the same throughout the reactor, an average conductivity was recorded over a 10 minute interval. Figure 16 shows the conversion versus temperature for both flow rates. As one can see, as the temperature was increased from 297 K, to 308 K, and then to 318 K, the conversion also increased from 0.7208 to 0.7849 and to 0.8231 respectively for the 60 mL/min flow rate, from 0.6364 to 0.6957 and to 0.7396 respectively for the 100 mL/min flow rate, and from 0.5639 to 0.6327 and to 0.6922 for the 140 mL/min flow rate. This was because the activation energy of the saponification reaction was a large, positive value. Because the temperature was rising between each step, the frequency of collisions was increases and thus the rate constant increased. As the rate constant increased for each of these temperatures, the conversion increased as well.

In general, the slower the feed streams are fed through the CSTR, the higher the conversion of the reaction is. Figure 16 and Figure 17 showed that the conversion increased as the residence time increased. This made sense because the residence time is inversely proportional to the

volumetric flow rates. As the flow rates increased, the residence time decreased, which resulted in the decrease of conversion.

The productivity of the old CSTR is shown in both Figure 18 and Figure 19. Figure 18 shows the effect of temperature versus productivity for both experimental sessions. As the temperature was increased, the productivity also increased (2.158E-5 to 2.350E-5 to 2.464E-5 mol/L*min for the 60 mL/min flow rate, 1.905E-3 to 2.083E-3 to 2.214E-3 mol/L*min for the 100 mL/min flow rate and 2.364E-3 to 2.901E-3 to 2.901E-3 mol/L*min for the 140 mL/min flow rate) for all three flow rates. This made sense because temperature caused an increase in the conversion, as previously stated. With an increase in conversion, more NaAc was formed in the same amount of time. However, when one takes into account the residence time in Figure 19, the productivity decreased as residence time increased. Once again, this made sense because the productivity measured the amount of product formed in a certain amount of time. So as the time decreased, the productivity increased.

Unlike the Batch Reactor, the concentration in the old CSTR is uniform and does not change with time. This allowed for the rate constant to be solved analytically for each recorded conductivity and then an average was taken. Since the rate constant was dependent on the conversion, as the temperature increased, the rate constant increased as well. The rate constant was used to calculate the activation energy by plotting the natural log of the rate constant versus 1/T. This resulted in a line that had a slope of -Ea/R. For the two experimental sessions with shorter residence times, the activation energies calculated were very similar: 31.86 kJ/mol and 33.79 kJ/mol. This was acceptable since the activation energy should have been the same or very close in both cases. Slight differences may have been caused from errors in the conductivity measurement or when steady-state was reached. However, the activation energy for largest residence time of 27.83 minutes resulted in an activation energy similar to that of the literature value (41.4 kJ.mol). This difference in activation energies for the residence times of 11.93 minutes and 16.7 minutes and the literature value, once again, could have been caused from errors in the conductivity measurement or from the lack of temperatures used. With more temperatures, there would have been more points used to determine the slope of -Ea/R, and therefore, resulted in an activation energy closer to 41.4 kJ/mol.

For the new CSTR, the overall conversions for both the single and series configurations were calculated at volumetric flow rates of 62 mL/min, 102 mL/min, and 152 mL/min. The data correctly proved that the overall conversion for a series configuration was greater than that of a single configuration at the same volumetric flow rate. At 62 mL/min, the overall conversion for the series configuration was 0.536 while the single configuration conversion was 0.458. For a volumetric flow rate of 102 mL/min, the series configuration and single configuration overall conversions were 0.466 and 0.403, respectively. The overall conversion at 152 mL/min for the series configuration was 0.417 while the conversion for the single configuration was 0.354. This pattern occurred because a CSTR operates at the exit concentrations, thus conversion does not vary with time inside the reactor. By using multiple reactors in series, the conversion approaches that of a PFR, giving the highest obtainable conversion at the same residence time.

The individual conversions for each reactor in the series configuration were also calculated at each volumetric flow rate. The data showed that for a given flow rate, the first reactor in the series had a higher conversion. At 62 mL/min, the first and second reactors had conversions of 0.381 and 0.251, respectively. For 102 mL/min, the first reactor had a conversion of 0.294 and the second had a conversion of 0.243. The conversion for the first reactor at 152 mL/min was 0.264 while conversion for the second reactor was 0.208. As previously stated, a CSTR operates at the exit concentrations, and so conversion was greater for the first reactor than for the second. The first reactor operated at a higher concentration than the second and had a higher rate of reaction, resulting in a higher conversion. The second reactor built on the conversion of the first to give a higher overall conversion than that of a single CSTR.

When the relationship between residence time and volumetric flow rate was examined, it was found that a higher flow rate led to a lower residence time. This was because volumetric flow rate is in the denominator of Equation 22. With an increased residence time, the reactants stayed in the reactor longer, thus leading to a higher conversion.

The overall productivities for both the single and series configurations were calculated at each volumetric flow rate. When comparing configurations, the productivity was greater for the series than for the single at all three volumetric flow rates. The productivity for the series configuration at 62 mL/min was 0.00208 mol NaAc/L*min while the productivity for the single configuration was 0.00177 mol NaAc/L*min. At 102 mL/min, the productivity for the series configuration was 0.00297 mol NaAc/L*min while it was 0.00257 mol NaAc/L*min for the single configuration. The productivities at 152 mL/min for the series configuration and single configuration were 0.00397 mol NaAc/L*min and 0.00336 mol NaAc/L*min, respectively. This was due to conversion being used in the numerator of Equation 22 to calculate productivity. The series configuration had a higher conversion than the single configuration, thus its productivity was higher.

Similar to the old and new CSTRs, residence time in the PFR decreased as flow rate increased, as shown in Figure 20. This result was plausible because as flow rate increased, the fluid moved much quicker through the reactor, experiencing a shorter residence time.

Conversion in the PFR increased as flow rate decreased, as a result of residence time. Since the smaller flow had a larger residence time, the reactants spent more time inside the reactor to form the desired product. The larger flow of 130 mL/min moved too quickly through the reactor to effectively form the product. The general trend showed a direct, increasing correlation between residence time and conversion.

Explained by kinetics, conversion was greater for the higher temperatures than for the lower temperatures. The kinetic rate of the reaction increased with increasing temperature. By increasing the temperature, the molecules moved faster and collided more often, thus increasing the reaction rate. The highest conversion achieved was 0.837, which occurred in the 80 mL/min flow rate trial at 45^{o}C. The lowest conversion was 0.429, which occurred in the 130 mL/min flow rate trial at room temperature (22^{o}C). In agreement with this, as temperature increased, the rate constant also increased. The maximum rate constants (0.274, 0.295, and 0.272 L/mol*sec) were found at the highest temperatures, and the lowest rate constants (0.0674, 0.0627, and 0.0652 L/mol*sec) were found at the lowest temperatures for the 80, 100, and 130

mL/min flow rates, respectively. Unexpectedly however, the rate constant k wasn't the same at each temperature for each trial. The largest flow rate, 130 mL/min, generally had the largest rate constant. Though, the differences between the rate constants were not very large. A possible explanation for this was that as the flow rate increased, the actual flow profile of the fluid became more thoroughly mixed, allowing for the reaction to take place quicker.

Once the rate constant value was determined for each trial and temperature, Figures 24, 25, and 26 were created by plotting ln(k) against 1/T. The figures were graphed this way so that the slope of the line would be equal to $-E_a/R$. From here, the activation energies were calculated to be 47.5, 52.6, and 48.7 kJ/mol for the 80, 100, and 130 mL/min mL/min flow rates, respectively. The average of these values was 49.6 kJ/mol, which was 8.2 kJ/mol larger than literature value for this reaction, 41.4 kJ/mol. This could be due to human error during the experiment. It was predicted that if the experiment was completed at several more temperatures, resulting in more data points on the activation energy graph, the activation energy found from the slope would be closer to the literature value for this reaction.

Productivity for this reaction was calculated once conversion, concentration of NaOH, and residence time were determined for each flow rate trial. Productivity was greatest for the 130 mL/min flow rate. The results showed that more product was made per given time in the 130 mL/min flow trial than in the other trials. This meant that the 130 mL/min flow trial was more efficient than the other flow trials, at creating product, even though its overall conversion was lower. Though the conversions were very close for each trial, the larger flow rate trial was more efficient since it took less time.

Overall, the best reactor condition for the saponification reaction would be a PFR operated at high temperatures. The PFR in the experimental sessions exhibited a productivity value of 0.00984 mol NaAc/L*min with a conversion of 0.815. For the old and new CSTRs, the highest productivity values were both below 0.00400 mol NaAc/L*min (0.00290 mol NaAc/L*min and 0.00397 mol NaAc/L*min, respectively). Theoretically, the batch reactor would have the highest conversion, as long as the cycle time was high enough.

However, unlike the batch reactor, the PFR is a continuous process. In order for the batch reactor to be employed for this process, the reactor would have to be filled and emptied manually after each batch, which would waste more time during the process (charging and discharging time).

Quality control would be another factor to consider. If the demanded product had to be pure, an impure product could easily be removed in a batch setting, since each batch is separate. However, if an impure product comes as a result of a PFR process, removing the impurities would be significantly more difficult, being continuous. Taking efficiency and quality control into consideration, the PFR at high temperatures would be the ideal reactor setup for this process.

Table 14 shows the statistical analysis for all of the experiments. In total, nine samples were used for each parameter: activation energy, k at room temperature, k at 35°C, and k at 45°C. This was taken into account when finding sample standard deviations. For our activation energies, the confidence interval contained the literature value, so we can assume that this analysis was consistent with actual industrial results. The confidence interval range increased for the rate constant as temperature increased, which makes sense since a higher temperature can increase the variance of these parameters. Through the analysis, it was found that the rate constant, on average, increased with temperature, which is consistent with the results in each individual experiment.

5.0 Summary and Conclusions

For the batch reactor evaluation, the technical objective was to find the relationships between conversion versus time, equilibrium conversion, reaction rate coefficient, and productivity against reaction temperature. It was found that as temperature increased, the time it took to reach a certain conversion decreased, indicating that the reaction was running at a higher rate. Equilibrium conversion decreased as temperature increased, but only slightly; the difference was so insignificant that the reaction could have been run at a higher temperature without compromising conversion. Reaction rate coefficients increased as temperature increased, in

accordance with the Arrhenius expression. The productivity also increased directly with temperature in the batch reactor setup.

For the old CSTR, the technical objectives were to calculate the steady-state conversion, rate constant, and productivity and to compare these to the residence time and temperature. As the temperature increased for both sessions, the conversion, rate constant, and productivity increased as well. Similarly, as the residence time increased, the conversion and rate constant increased, but the productivity decreased. For the highest productivity, it was found that the optimum temperature and residence time to run the old CSTR were at 45°C and 11.93 minutes.

The goal of the new CSTR experiment was to determine the effects of flow rate and configuration type on conversion and productivity. When the experiment was conducted at a higher flow rate, the productivity increased while the conversion decreased. The series configuration gave a higher productivity and a higher overall conversion than the single configuration at all three flow rates. The second reactor in the series built on the conversion of the first reactor. As more reactors are added in series, the overall conversion becomes closer to that of a PFR.

The technical objective for the PFR was to evaluate how reactor temperature and residence time affects steady-state conversion, reaction rate coefficient, and reaction productivity. As seen in the figures before, the trend for higher conversion was apparent as both temperature and residence time were increased. In order to maximize conversion, the ideal PFR reactor would be operated at a high temperature and a moderate to low residence time. However, productivity was greater in the PFR for the smaller residence time.

Conversion, reaction time, and quality control are important elements to consider when choosing a reactor. From the data and results, a PFR run at high temperatures would be best for this saponification reaction.

6.0 References

[1] "Batch Reactors." *Batch Reactors*. University of Michigan, n.d. Web. 16 Mar. 2017. <http://umich.edu/~elements/asyLearn/bits/batch/index.htm>.

[2] Das. Sahoo. Magapu. Swaminathan. “Thermodynamic Parameters in Saponification Reaction” *International Journal of Chemical Kinetics* Vol. 43, November 2011.

7.0 Appendix

7.1 Appendix – Sample Calculations

7.1.1 Thermodynamic Analysis

The heat of reaction was found using literature values of standard heats of formation. This was done using a products-minus-reactants formula, giving

$$\Delta H_R = (\Delta H_{NaAc} + \Delta H_{EtOH}) - (\Delta H_{NaOH} + \Delta H_{EtAc}) \qquad \text{Equation 1}$$

$$\Delta H_R = \left(-709.3\frac{kJ}{mol} - 277.7\frac{kJ}{mol}\right) - \left(-427.0\frac{kJ}{mol} - 479.0\frac{kJ}{mol}\right) = -81.0\frac{kJ}{mol}.$$

A similar calculation was done to find the standard Gibbs free energy change of reaction, with

$$\Delta G_R = (\Delta G_{NaAc} + \Delta G_{EtOH}) - (\Delta G_{NaOH} + \Delta G_{EtAc}), \qquad \text{Equation 2}$$

$$\Delta G_R = \left(-607.7\frac{kJ}{mol} - 174.1\frac{kJ}{mol}\right) - \left(-380.7\frac{kJ}{mol} - 332.7\frac{kJ}{mol}\right) = -68.4\frac{kJ}{mol}.$$

These values were constant throughout the rest of the calculations for the thermodynamic analysis. The calculations that follow are for the room temperature scenario (22°C).

K_{eq} was found using

$$K_{eq} = \exp\{\frac{-\Delta G_R}{R*T}\}. \qquad \text{Equation 3}$$

At 22°C, this equation becomes

$$K_{eq} = \exp\left\{\frac{68{,}400\frac{J}{mol}}{8.314\frac{J}{mol*K}*295\ K}\right\} = 1.29357 * 10^{12}. \qquad \text{Equation 4}$$

The equilibrium conversion, X_{eq}, was found using

$$K_{eq} = (\frac{X_{eq}}{1-X_{eq}})^2. \qquad \text{Equation 5}$$

Using Excel's Solver feature and inputting the calculated $K_{eq,}$ the equilibrium conversion at 22°C becomes

$$X_{eq} = 0.999999121.$$

7.1.2 Batch

In order to gain conversion data from the batch experiments, corrected lambda values needed to be calculated to account for the slight changes in temperature that may have occurred throughout the trial. The following calculations relate to the first experimental session, at room temperature (22°C), ten seconds into the reaction.

Corrected lambda values for NaOH and NaAc were found using

$$\lambda_{NaOH} = \frac{\kappa_{NaOH,std} + \alpha_{NaOH}(T - T_{NaOH,std})}{C_{NaOH,std}}, \quad \text{Equation 6}$$

$$\lambda_{NaAc} = \frac{\kappa_{NaAc,std} + \alpha_{NaAc}(T - T_{NaAc,std})}{C_{NaAc,std}}. \quad \text{Equation 7}$$

Using standardized values and the temperature at ten seconds, those equations become

$$\lambda_{NaOH} = \frac{21.3\ mS + 0.386\frac{mS}{C}(22.3C - 20.6C)}{0.1\frac{mol}{L}} = 219.6\frac{mS*L}{mol},$$

$$\lambda_{NaAc} = \frac{6.4\ mS + 0.164\frac{mS}{C}(22.3C - 20.6C)}{0.1\frac{mol}{L}} = 66.8\frac{mS*L}{mol}.$$

These values were used to find the conversion of NaOH at a certain time. The equation for the conductivity of the solution with respect to concentrations is

$$\kappa = (\lambda_{NaOH} \times C_{NaOH}) + (\lambda_{NaAc} \times C_{NaAc}). \quad \text{Equation 8}$$

Each of the concentrations can be redefined to find conversion relationships for NaOH. Namely,

$$C_{NaOH} = (1 - X)C_{NaOH,o}, \quad \text{Equation 9}$$

$$C_{NaAc} = (X)C_{NaOH,o}. \quad \text{Equation 10}$$

Substituting these relationships into Equation 8 and solving for X gives

$$X = \frac{\kappa}{C_{NaOH,o}(\lambda_{NaAc} - \lambda_{NaOH})} - \frac{\lambda_{NaOH}}{\lambda_{NaAc} - \lambda_{NaOH}}. \quad \text{Equation 11}$$

Substituting the respective values at ten seconds can find the conversion at that time:

$$X = \frac{9.74\ mS}{0.05\frac{mol}{L}(66.8\frac{mS*L}{mol} - 219.6\frac{mS*L}{mol})} - \frac{219.6\frac{mS*L}{mol}}{\left(66.8\frac{mS*L}{mol} - 219.6\frac{mS*L}{mol}\right)} = 0.1621.$$

The rate law for this saponification reaction is

$$\frac{d}{dt}(C_{NaOH}) = (r_{NaOH}) = -k_r C_{EtOH} C_{NaAc} + k_f C_{EtAc} C_{NaOH}.$$

Since K_{eq} is so large for this reaction, the reverse reaction can be assumed to have no contribution to the rate law. In other words, k_r can be assumed to be zero. The rate law then simplifies to

$$\frac{d}{dt}(C_{NaOH}) = (r_{NaOH}) = k_f C_{EtAc} C_{NaOH}.$$

After integrating, the equation becomes

$$\frac{1}{C_{NaOH}} - \frac{1}{C_{NaOH,o}} = k * t. \quad \text{Equation 12}$$

Therefore, plotting the left side of the equation against time allows us to find the rate coefficient for the reaction. To ensure a good linear fit and to reduce volatility issues in the solution, only the first three minutes of the experiment were used for analysis. The plot is given in Figure 30. The slope of the line of best fit is assumed to be the rate coefficient (for the room temperature reaction).

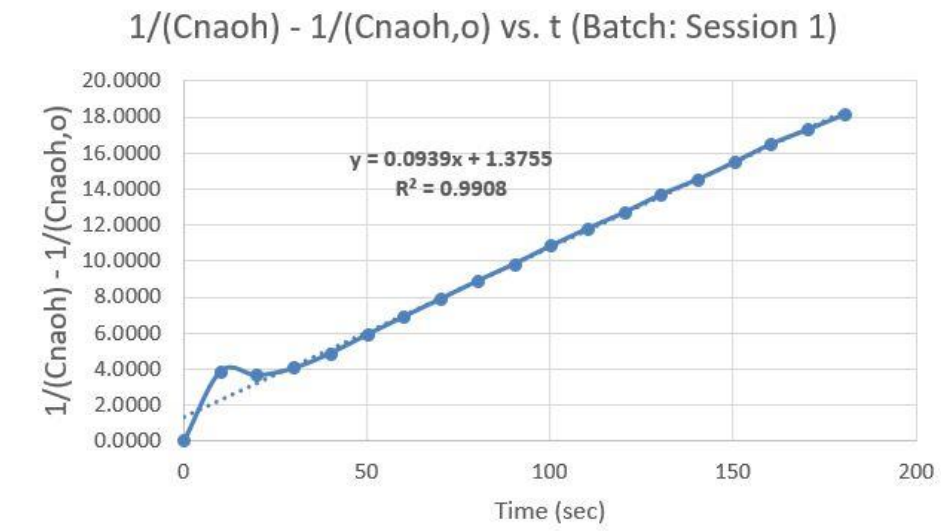


Fig. 30. Plot used to find the Reaction Rate Coefficient (Session 1: Room Temperature)

The relationship between the rate coefficient and activation energy is described by the Arrhenius equation:

$$k = k_o \exp(\frac{-E_a}{R*T}). \qquad \text{Equation 13}$$

To linearize the equation, taking the natural log of both sides gives

$$\ln(k) = \frac{-E_a}{R*T} + \ln(k_o).$$

Therefore, when plotting ln(k) against 1/T, the activation energy can be found by multiplying the slope of the fitted line by the negative ideal gas constant. The plot used for the first session's activation energy calculation is shown in Figure 31.

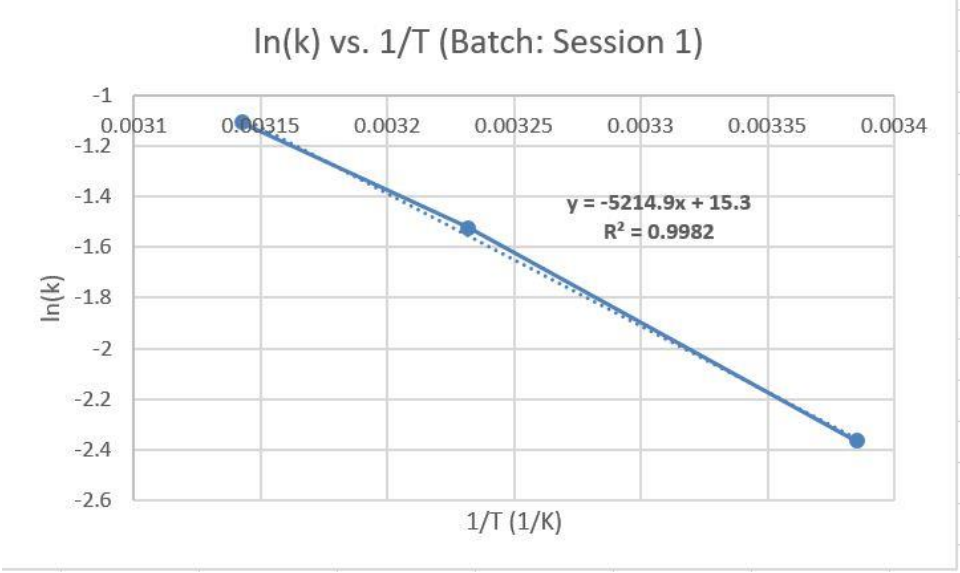


Fig. 31. Plot used to find Activation Energy (Session 1)

From the plot, one can see that the slope is –5214.9 K. The activation energy was found using

$$E_a = -\left(8.314 \frac{J}{mol*K}\right) * (-5214.9\ K) * \left(\frac{1\ kJ}{1000\ J}\right) = 43.357 \frac{kJ}{mol}.$$

The equation used to find productivity is

$$P = \frac{C_{NaOH,o} X}{Cycle\ Time}. \qquad \text{Equation 14}$$

Where Cycle Time is defined as

$$Cycle\ Time = Charging\ Time + Reaction\ Time + Discharch\ Time. \qquad \text{Equation 15}$$

Simultaneous charging time was found by

$$Charging\ Time = \frac{V_{NaOH}}{Charging\ Rate} = \frac{500\ mL}{100\ (\frac{mL}{min})} = 5\ min.$$

Reaction time was found by finding the time it took for the reaction to reach 60% conversion. In the case of the first experimental session, this was reached around 320 seconds (5.33 min) into the batch experiment (at room temperature).

Discharge time was found by

$$Discharge\ Time = \frac{V_{NaOH}+V_{EtAc}}{Discharging\ Rate} = \frac{1000\ mL}{200\ (\frac{mL}{min})} = 5\ min. \quad \text{Equation 16}$$

Therefore,

$$Cycle\ Time = (5\ \text{min}) + (5.33\ \text{min}) + (5\ \text{min}) = 15.33\ \text{min}.$$

Therefore, productivity for the first batch session at room temperature was

$$P = \frac{C_{NaOH,o}X}{Cycle\ Time} = \frac{\left(0.05\frac{mol}{L}\right)*0.6}{15.33\ min} = 0.00195652\frac{mol\ NaAc}{L*\text{min}}.$$

7.1.3 Old CSTR

7.1.3.a. Specific Conductance

$$\lambda_{NaOH} = \frac{K_{NaOH,STD} + \propto_{NaOH} * (T - T_{STD})}{C_{NaOH,STD}} \quad \text{Equation 17}$$

$$\lambda_{NaOH} = \frac{21.3\ mS + 0.3317\frac{mS}{℃} * (24.257 - 21.2)℃}{0.1\frac{mol}{L}} = 223.14\ mS * L/mol$$

$$\lambda_{NaAc} = \frac{6.52\ mS + 0.1787\ \frac{mS}{℃} * (24.257 - 21.2)℃}{0.1\frac{mol}{L}} = 70.66\ mS * L/mol$$

The specific conductance was also calculated for NaAc in a similar fashion as the specific conductance was calculated for NaOH.

$$\lambda_{NaAc} = 70.66\ mS * L/mol$$

7.1.3.b. Conversion

To find the conversion, the specific conductance of both NaOH and NaAc were used as well as the measured conductance of the solution.

$$X = \frac{K}{C_{NaOH,o} * (\lambda_{NaAc} - \lambda_{NaOH})} \frac{\lambda_{NaOH}}{(\lambda_{NaAc} - \lambda_{NaOH})} \qquad \text{Equation 18}$$

$$X = \frac{6.332\ mS}{0.05 \frac{mol}{L} * (70.66 - 223.14)\ mS * L/mol} - \frac{223.14\ mS * \frac{L}{mol}}{(70.66 - 223.14)\ mS * \frac{L}{mol}} = 0.6329$$

7.1.3.c. Residence time

The example calculation for residence time was calculated for the first experimental session where the flow rates of both species were added together for the total flow rate of 100 mL/min.

$$\tau = \frac{V}{\dot{\upsilon}} \qquad \text{Equation 19}$$

$$\tau = \frac{1670\ mL}{100\ \frac{mL}{min}} * \frac{60\ s}{min} = 1002\ s$$

The residence time was also calculated for the second experimental session where the volumetric flow rate increased to 140 mL/min.

The specific conductance, the conversion, and the rate constant example calculations are for the first experimental session and the first recorded data set of the room temperature measurement.

7.1.3.d. Rate Constant

The rate constant was then calculated using the following equation:

$$k_f = \frac{X}{\tau * C_{NaOH,o} * (1 - X)^2} \qquad \text{Equation 20}$$

$$k_f = \frac{0.6329}{1002\ s * 0.05 \frac{mol}{L} * (1 - 0.6329)^2} = \frac{0.0937 L}{mol * s}$$

Since the data was taken at steady-state over a ten minute time interval, the following calculations were repeated and the average conversion and rate constant were recorded. These steps were also used for 35°C and 45°C of the first experimental session as well as the same three temperatures the experiment was run at for the second experimental session.

7.1.3.e. Activation Energy

The activation energy was calculated by plotting ln(k) versus 1/T for each of the three temperatures. The slope of the line formed from these three points in excel and shown in Fig. 32 and Fig. 33.

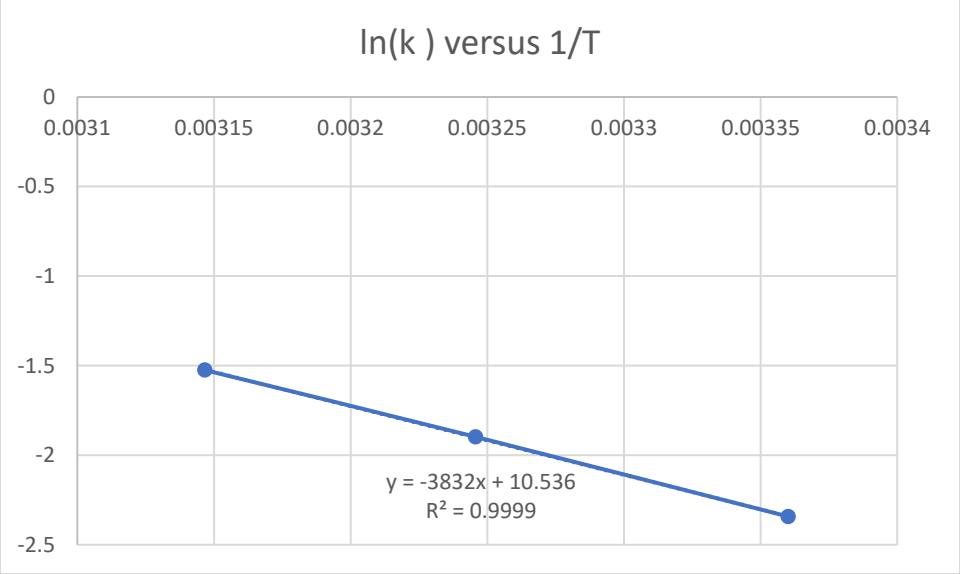


Fig. 32. Plot of ln(k) versus 1/T to determine Ea for τ = 16.7 min.

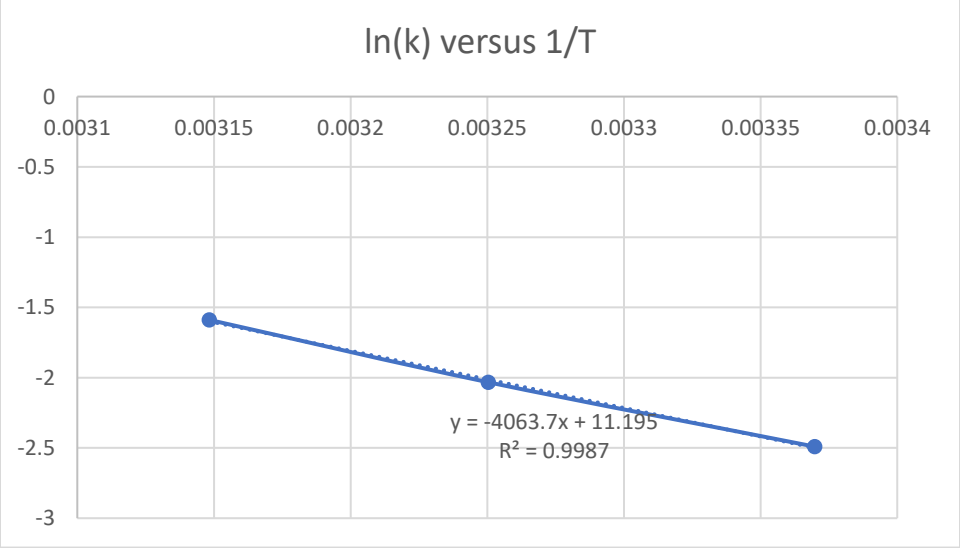


Fig. 33. Plot of ln(k) versus 1/T to determine Ea for τ = 11.93 min.

$$Slope = \frac{E_A}{R} \qquad \text{Equation 21}$$

$$E_A = Slope * R = 3832 * 8.314 \frac{J}{mol * K} = 31.86 \frac{kJ}{mol * K}$$

Similarly, the activation energy was calculated when the residence time decreased to 11.93 min in the second experimental session.

7.1.3.f. Productivity

To solve for the productivity, the following equation was used:

$$P = \frac{X * C_{NaOH,o}}{\tau} \qquad \text{Equation 22}$$

For the first experimental session at room temperature, the productivity was calculated as followed:

$$P = \frac{0.6364 * 0.05 \frac{mol}{L}}{1002\ s} * \frac{60\ s}{min} = 0.00191\ mol\ NaAc/(L * \text{min})$$

7.1.4 New CSTR

7.1.4.a. Conductance

Specific conductance for NaOH

$$\lambda_{NaOH} = \frac{\kappa_{NaOH,std} + \alpha_{NaOH,std}(T - T_{NaOH,std})}{C_{NaOH,std}}$$

$$= \frac{(20.2\ mS)(10^{-3}) + \left(0.4074\ \frac{mS}{°C}\right)(10^{-3})(22.2°C - 20.6°C)}{(0.5)\left(0.1 \frac{mol}{L}\right)} = 0.2085 \frac{L * S}{mol}$$

Specific conductance for NaAc

$$\lambda_{NaAc} = \frac{\kappa_{NaAc,std} + \alpha_{NaAc,std}(T - T_{NaAc,std})}{C_{NaAc,std}}$$

$$= \frac{(6.05\,mS)(10^{-3}) + \left(0.1933\ \frac{mS}{℃}\right)(10^{-3})(22.2℃ - 20.3℃)}{(0.5)(0.1\frac{mol}{L})} = 0.0642\frac{L*S}{mol}$$

7.1.4.b. Conversion

Conversion for single CSTR (also used for individual conversion of 1st CSTR in series)

$$X_{single} = \frac{\kappa}{C_{NaOH,0}(\lambda_{NaAc} - \lambda_{NaOH})} - \frac{\lambda_{NaOH}}{(\lambda_{NaAc} - \lambda_{NaOH})}$$

$$= \frac{(7.87\,mS)(10^{-3})}{(0.5)\left(0.1\ \frac{mol}{L}\right)\left(0.0642\ \frac{L*S}{mol} - 0.2085\ \frac{L*S}{mol}\right)}$$

$$- \frac{\left(0.2085\ \frac{L*S}{mol}\right)}{\left(0.0642\ \frac{L*S}{mol} - 0.2085\ \frac{L*S}{mol}\right)} = 0.3541$$

Calculation of individual conversion for 2nd CSTR in series

$$X_2 = \frac{\kappa - \lambda_{NaOH}C_{NaOH,1} - \lambda_{NaAc}C_{NaAc,1}}{\lambda_{NaAc}C_{NaOH,1} - \lambda_{NaOH}C_{NaOH,1}}$$

$$= \frac{(7.35\,mS)(10^{-3}) - \left(0.2069\ \frac{L*S}{mol}\right)\left(0.03678\ \frac{mol}{L}\right) - (0.0634\ \frac{L*S}{mol})(0.01322\ \frac{mol}{L})}{\left(0.0634\ \frac{L*S}{mol}\right)\left(0.03678\ \frac{mol}{L}\right) - (0.2069\ \frac{L*S}{mol})(0.03678\ \frac{mol}{L})}$$

$$= 0.2079$$

Calculation of overall conversion of two CSTRs in series

$$X_{overall} = \frac{C_{NaOH,0} - C_{NaOH,2}}{C_{NaOH,0}} = \frac{(0.5)\left(0.1\frac{mol}{L}\right) - \left(0.02913\ \frac{mol}{L}\right)}{(0.5)\left(0.1\frac{mol}{L}\right)} = 0.4174$$

7.1.4.c Concentration

Calculation of $C_{NaOH,1}$ using conversion from 1st CSTR in series

$$C_{NaOH,1} = C_{NaOH,0}(1 - X_1) = (0.5)\left(0.1\ \frac{mol}{L}\right)(1 - 0.2644) = 0.03678\ \frac{mol}{L}$$

Calculation of $C_{NaAC,1}$ using conversion from 1st CSTR in series

$$C_{NaAc,1} = C_{NaOH,0}X_1 = (0.5)\left(0.1\ \frac{mol}{L}\right)(0.2644) = 0.01322\ \frac{mol}{L}$$

Calculation of $C_{NaOH,2}$ using conversion from 2nd CSTR in series

$$C_{NaOH,2} = C_{NaOH,1}(1 - X_2) = \left(0.03678\ \frac{mol}{L}\right)(1 - 0.2079) = 0.02913\ \frac{mol}{L}$$

7.1.4.d Residence Time

Calculation of residence time for single CSTR

$$\tau_{single} = \frac{V_{single}}{F_{single}} = \frac{0.8\ L}{(2)(76\ \frac{mL}{min})(10^{-3})} = 5.263\ min$$

7.1.4.e. Calculation of $\tau_{overall}$ for two CSTRs in series

$$\tau_{overall} = \frac{V_1}{F_1} + \frac{V_2}{F_2} = \frac{(0.4\ L)}{(2)(76\ \frac{mL}{min})(10^{-3})} + \frac{(0.4\ L)}{(2)(76\ \frac{mL}{min})(10^{-3})} = 5.263\ min$$

7.1.4.f. Productivity

Calculation of productivity for single CSTR

$$P_{single} = \frac{C_{NaOH,0}X_{single}}{\tau_{single}} = \frac{(0.5)\left(0.1\ \frac{mol}{L}\right)(0.3541)}{5.263\ min^{-1}} = 0.00336\ \frac{mol\ NaAc}{L * min}$$

Calculation of overall productivity for two CSTRs in series

$$P_{overall} = \frac{C_{NaOH,0} X_{overall}}{\tau_{overall}} = \frac{(0.5)(0.1\ \frac{mol}{L})(0.4174)}{\frac{(0.4\ L)}{(2)(76\ \frac{mL}{min})(10^{-3})} + \frac{(0.4\ L)}{(2)(76\ \frac{mL}{min})(10^{-3})}}$$

$$= 0.003965\ \frac{mol\ NaAc}{L * min}$$

7.1.5 PFR

7.1.5.a. Specific Conductance

$$\lambda_{NaOH} = \frac{K_{NaOH,std} + \alpha_{NaOH}(T - T_{NaOH,std})}{C_{NaOH,std}} = \frac{19.5\ mS\ + .4233 mS/^{o}C(45^{o}C - 21.1^{o}C)}{0.1\ M}$$

$$= 296.1687\ mSL/mol$$

$$\lambda_{NaAc} = \frac{K_{NaAc,std} + \alpha_{NaAc}(T - T_{NaAc,std})}{C_{NaAc,std}} = \frac{5.87\ mS\ + .1585 mS/^{o}C(45C - 20.5^{o}C)}{0.1\ M}$$

$$= 97.5325\ mSL/mol$$

7.1.5.b. Conversion

$$X = \frac{K}{C_{NaAc,std}(\lambda_{NaAc} - \lambda_{NaOH})} - \frac{\lambda_{NaOH}}{\lambda_{NaAc} - \lambda_{NaOH}}$$

$$= \frac{6.75\ mS}{0.05M(97.5325 - 296.1687\ mSL/mol} - \frac{296.1687\frac{mSL}{mol}}{97.5325 - 296.1687\frac{mSL}{mol}} =$$

$$= 0.811$$

7.1.5.c. Residence time

$$\tau = \frac{V}{\dot{V}} = \frac{1000\ mL}{2 * 100\ mL/min} = 5\ min$$

7.1.5.d. Rate Constant

$$k = \frac{\dot{V}}{V}\left(\frac{1}{C_{NaOH}} - \frac{1}{C_{NaOH,o}}\right) = \frac{2 * 100mL/min}{1000\ mL}\left(\frac{1}{.00943\ M} - \frac{1}{.05\ M}\right) = .2867\frac{L}{molS}$$

7.1.5.e. Activation Energy

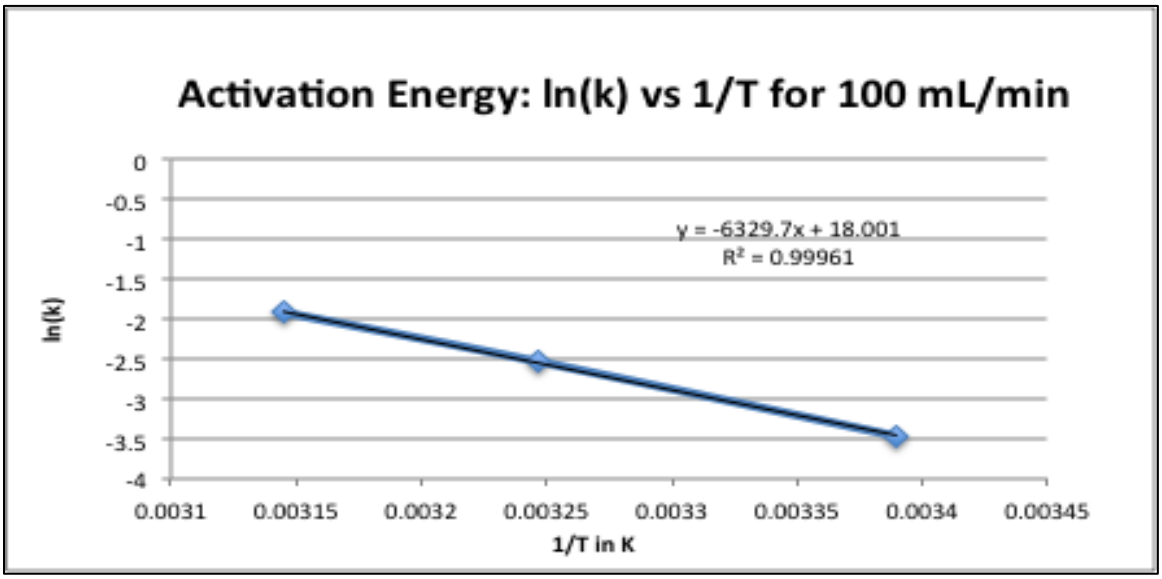


Fig. 34. Plot to calculate activation energy from slope for PFR.

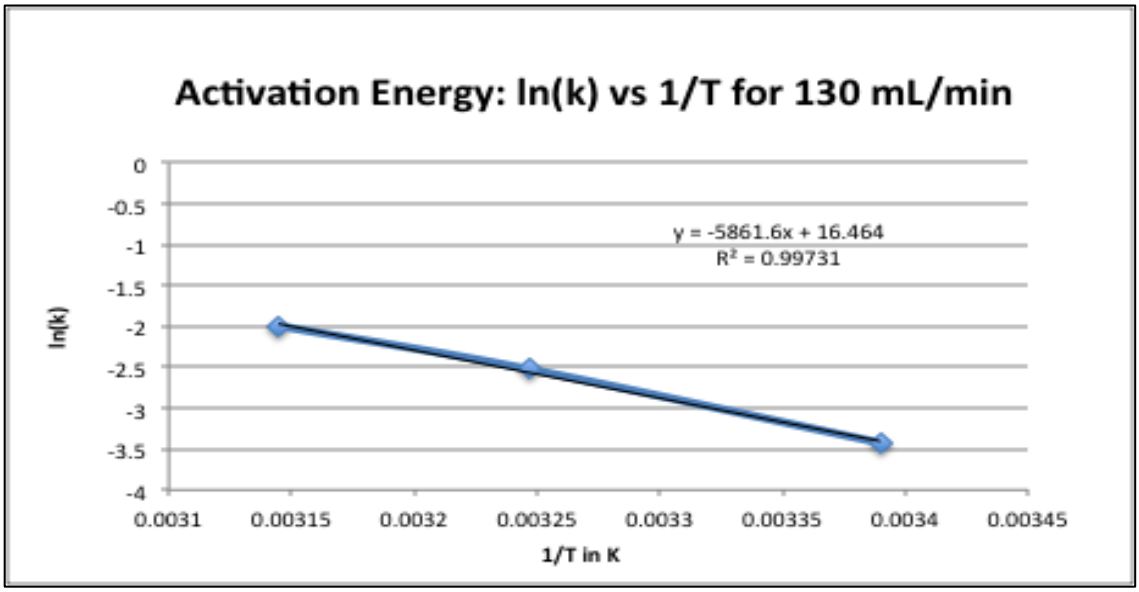


Fig. 35. Plot to calculate activation energy from slope for PFR.

$$E_a = \frac{-slope * R}{1000J/kJ} = \frac{-6329.7 * 8.314J/molK}{1000J/kJ} = 52.62\ kJ$$

7.1.5.f. PFR Equations:

$$u\frac{d}{dz}C_{NaOH} = (r_{NaOH)} \qquad \text{Equation 23}$$

$$k = \frac{u}{L} * \left(\frac{1}{C_{NaOH}} - \frac{1}{C_{NaOH,o}}\right) = \frac{\dot{V}}{V} * \left(\frac{1}{C_{NaOH}} - \frac{1}{C_{NaOH,o}}\right) \qquad \text{Equation 24}$$

7.1.5.g. Productivity

$$P = \frac{X * C_{NaOH}}{\tau} = \frac{.811 * .05M}{5\ min} = .00811\ M/min \qquad \text{Equation 25}$$